Articles

Structure−Activity Relationships of the Antimalarial Agent Artemisinin. 8. Design, Synthesis, and CoMFA Studies toward the Development of Artemisinin-Based Drugs against Leishmaniasis and Malaria†

Mitchell A. Avery,*,‡,§ Kannoth M. Muraleedharan,‡ Prashant V. Desai,‡ Achintya K. Bandyopadhyaya,‡ Marise M. Furtado,|| and Babu L. Tekwani||

Department of Medicinal Chemistry, School of Pharmacy, National Center for Natural Products Research, and Department of Chemistry, University of Mississippi, University, Mississippi 38677

Received April 17, 2003

Artemisinin (**1**) and its analogues have been well studied for their antimalarial activity. Here we present the antimalarial activity of some novel C-9-modified artemisinin analogues synthesized using artemisitene as the key intermediate. Further, antileishmanial activity of more than 70 artemisinin derivatives against *Leishmania donovani* promastigotes is described for the first time. A comprehensive structure−activity relationship study using CoMFA is discussed. These analogues exhibited leishmanicidal activity in micromolar concentrations, and the overall activity profile appears to be similar to that against malaria. Substitution at the C-9β position was shown to improve the activity in both cases. The 10-deoxo derivatives showed better activity compared to the corresponding lactones. In general, compounds with C-9α substitution exhibited lower antimalarial as well as antileishmanial activities compared to the corresponding C-9β analogues. The importance of the peroxide group for the observed activity of these analogues against leishmania was evident from the fact that 1-deoxyartemisinin analogues did not exhibit antileishmanial activity. The study suggests the possibility of developing artemisinin analogues as potential drug candidates against both malaria and leishmaniasis.

Introduction

Artemisinin (**1**), a sesquiterpene endoperoxide isolated from the plant *Artemisia annua*, has emerged as an important treatment option toward drug-resistant strains of *Plasmodium falciparum*.[1,2] After its isolation in 1972 by Chinese researchers and structure elucidation in 1979,[3] artemisinin became the center of attention for drug development against drug-resistant malaria. It has been shown to quickly lower the parasite levels even in severe cases of cerebral malaria. Artemisinin (**1**) has demonstrated activity against drug-resistant strains of *P. falciparum* such as W2-Indochina (chloroquine resistant) and D6-Sierra Leone (mefloquine resistant) clones. The mechanism of action of this unusual 1,2,4-trioxane is believed to involve an initial interaction of the endoperoxide moiety with heme, resulting in the formation of free radical intermediates.[4−12] The exact mechanism by which these free radicals cause parasitic death is still not completely understood.[13,14] Recently much attention has been given to the chemical modification of artemisinin in order to improve its efficacy and pharmaceutical profile.[15−22] Artemisinin derivatives such as artesunate and arteether, either alone or in combination with other drugs, are being used as a remedy for malaria in many endemic areas.[23] Although several C-10 ether derivatives of dihydroartemisinin are in clinical use against malaria, poor oral bioavailability, short plasma half-life, and concerns regarding neurotoxicity limit their use.[24]

Artemisinin and its analogues have also been studied for their anticancer,[25−30] and antifungal action.[31,32] Our search for reports on the action of artemisinin against other diseases caused by parasites related to *P. falciparum*, like trypanosomiasis and leishmaniasis, resulted in only one relevant study in which its activity against leishmania was described.[33] Although it was a preliminary finding, it did suggest a possible use of artemisinin and related analogues against leishmaniasis.

Human leishmaniasis comprises a heterogeneous spectrum of diseases. Three major forms are generally distinguished: cutaneous leishmaniasis, mucocutaneous leishmaniasis, and visceral leishmaniasis, of which the latter is potentially lethal. They are caused by various species of the protozoan parasite *Leishmania* and transmitted by female sandflies.[34] The disease is currently proposed to affect some 12 million people in 88 countries.[35−39] It is estimated that ∼350 million people are exposed to infection by different species of leishma-

† This paper is dedicated to Dr. Jeffrey A. Vroman[45] (deceased Jan 2003).

* To whom correspondence should be addressed. Phone: (662)-915-5879. Fax: (662)-915-5638. E-mail: mavery@olemiss.edu.

‡ Department of Medicinal Chemistry, University of Mississippi.

§ Department of Chemistry, University of Mississippi.

|| National Center for Natural Product Research, University of Mississippi.

10.1021/jm030181q CCC: $25.00
Published on Web 08/21/2003

Scheme 1

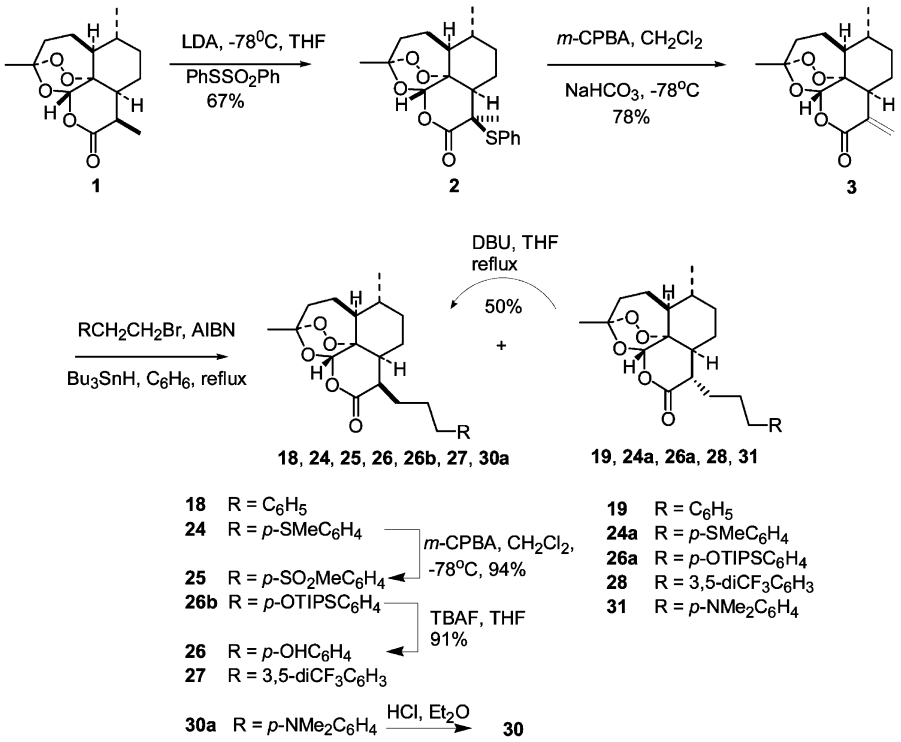

nia parasite. Leishmania/HIV coinfection is now considered as an "emerging disease" especially in southern Europe, where 25−70% of adult visceral leishmaniasis cases are related to HIV infection.

The current treatment for leishmaniasis involves administration of pentavalent antimony complexed to a carbohydrate in the form of sodium stibogluconate (pentosam or Sb(V)) or meglumine antimony (glucantine), which are the only antileishmanial chemotherapeutic agents with a reasonable therapeutic index.[40,41] The exact chemical structure and mode of action of pentavalent antimonials is still uncertain but, as with most metals, is thought to be multifactorial.[41] Amphotericin B and pentamidine are the second line of antileishmanial agents, but they are reserved for nonresponding infections due to potential toxicity.[42] The development of lipid-associated amphotericin B provided important clinical progress in this area.[43,44] Even though many promising leads exist, none of the above-mentioned drugs show promise as ideal treatment alternatives for the developing world, due to their route of administration (parenteral), high clinical failure rate (40% for pentavalent antimonial agents), side effects, and cost. Thus, the identification of an effective antileishmanial agent for oral administration would be a significant step toward reducing mortality due to leishmaniasis.

Our ongoing program to develop artemisinin-based antimalarial drugs, coupled with possible activity against leishmania, prompted us to explore the possibility of designing and developing artemisinin analogues having both antimalarial and leishmanicidal activity.

Comparative molecular field analysis of over 200 artemisinin analogues from this laboratory has shown important electrostatic and steric requirements that could improve the antimalarial activity of the artemisinin skeleton.[45d] Steric bulk in the form of phenethyl substitution at C-9β and the removal of the carbonyl group to form the 10-deoxo system have been shown to give optimal oral activity. On this basis, we have modified the C-9 position of the parent skeleton with various aliphatic and arylalkyl groups. The most promising candidates were those with a halogen-substituted phenethyl group at the C-9 position. However, oral bioavailability of most of these molecules was comparatively low.[46a]

In this paper we present the antimalarial activity of some novel artemisinin analogues. Also, we report the first comprehensive structure−activity relationship study of more than 70 artemisinin analogues against leishmania promastigotes using comparative molecular field analysis (CoMFA).

Chemistry

The synthesis of new artemisinin derivatives, which are expected to have improved bioavailability, is presented in Scheme 1. A selenium-free route to artemisitene (**3**) was employed, after which **3** was then reacted with the appropriate arylalkyl bromide synthons. For radical-induced Michael addition of artemisitene, a dilute solution of tributyltin hydride was added slowly over 8 h, via syringe pump, to a refluxing solution of artemisitene, AIBN, and the corresponding bromide. The solvent was concentrated to 25 mL, stirred with a saturated solution of KF for 10 h, filtered, and concentrated. The products were separated by column chromatography to afford the α- and β-epimers. Yield of the β-isomer ranged from 14% to 32% and that of α-isomer from 30% to 43%. The 9α-substituted analogues were converted to the 9β-congeners by refluxing with DBU in THF for 12 h. Table 1 shows the yields of α- and β-isomers prior to equilibration.

As shown in Scheme 2, the bromide synthons used (**6a**−**c**) were synthesized from the corresponding acids

Scheme 2

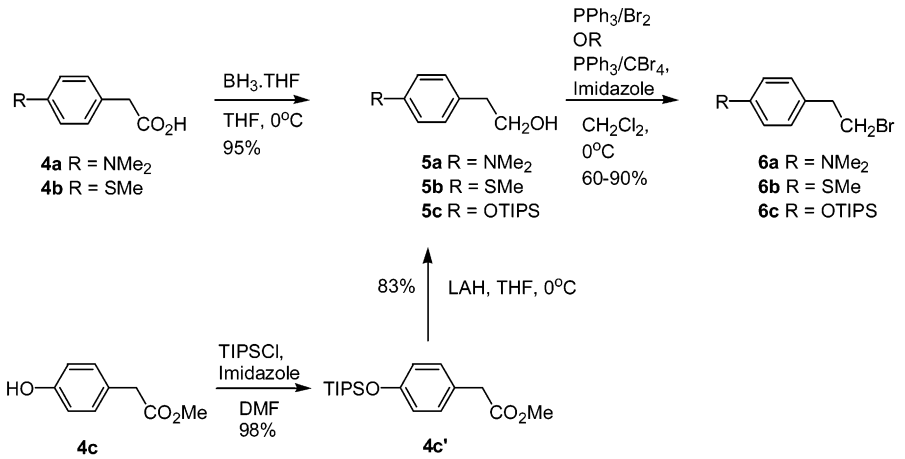

Table 1. Percentage Yields of α- and β-Diastereomers Prior to Equilibration as Described in Scheme 1

β-isomers		α-isomers	
compd	% yield	compd	% yield
15	14 (29)[a]	**15a**	35
18[b] (R = Ph)	21 (24)[a]	**19**	30
24 (R = SMe)	17 (33)[a]	**24a**	38
26b (R = OTIPS)	22[c]	**26a**	39
27[b] (R = 3,5-diCF$_3$)	32 (45)[a]	**28**	43
30a (R = NMe$_2$)	30 (42)[a]	**31**	32

[a] Numbers in parentheses represent the combined yield of C-9β isomers after one round of DBU epimerization of α-diastereomer. [b] The analytical data of these compounds are described in ref 46a. [c] Not subjected to equilibration.

Table 2. Antimalarial Activity of New Artemisinin Analogues[a]

	P. falciparum IC$_{50}$ (nM)			*P. falciparum* IC$_{50}$ (nM)	
no.	D6 clone	W2 clone	no.	D6 clone	W2 clone
15	14.9	14.9	**28**	12.6	8.2
18	4.7	1.3	**30**	27.8	11.3
19	10.4	3.4	**31**	38.7	62.3
24	43.9	50.8	**55**	16.5	14.3
25	30.13	20	artemisinin	17.0	14.5
26	7.9	4.7	chloroquine	16.5	232.6
27	18.8	16	mefloquine	169.5	194.6

[a] Activity was measured using the pLDH assay as described in text.[47] All the analogues were tested at least at six different concentrations, each in duplicate. The mean values were used to generate the growth inhibition curves and determination of IC$_{50}$ values.

Scheme 3

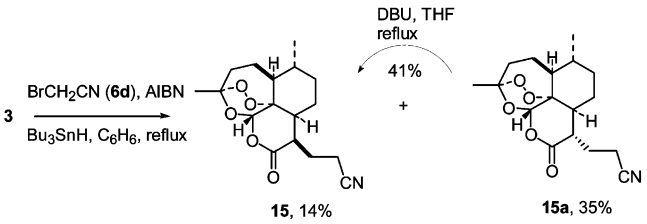

first by reduction to alcohols followed by bromination using PPh_3/CBr_4 (for **6a**) or PPh_3/Br_2 (for **6b** and **6c**).

The synthesis of C-9 cyanoethyl derivative of artemisinin (**15**) is presented in Scheme 3. Here, bromoacetonitrile (**6d**) was used in the Michael addition to artemisitene to afford the β-isomer **15** and α-isomer **15a** in 14% and 35% yields, respectively. As described previously, the α-isomer was converted to the β-form in 41% yield, by refluxing with DBU in THF for 10 h.

The 10-deoxo derivative **55a** was synthesized from compound **30a** in 35% yield using a two-step reaction sequence involving two reductions, first affording the lactol (**30b**) in 82% yield, followed by a second reduction with triethylsilane and boron trifluoride etherate (Scheme 4). Due to the potential instability of the peroxide group in the presence of the amino function,[12b] the *N*,*N*-dimethylamino derivatives **30a** and **55a** were converted to the corresponding hydrochloride salts by treatment with equimolar amounts of HCl in ether. The formation of hydrochloride salts was evidenced by the shift of ^{1}H NMR signals corresponding to the NMe$_2$ groups from δ 2.9 to 3.14 and that of aromatic doublets from δ 6.69 and 7.04 to δ 7.28 and 7.65, respectively. The conversion of sulfide (**24**) to sulfone (**25**) was accomplished in 94% yield by treatment with *m*-CPBA at −78 °C in CH_2Cl_2. Similarly, the silyl group in **26b** could be removed conveniently using tetrabutylammonium fluoride in THF, at room temperature to afford 91% of **26**. Most of the newly synthesized artemisinin analogues exhibited superior antimalarial activities compared to artemisinin, as described in Table 2.

All the other compounds studied in this report and listed in Tables 3 and 4 were retrieved from library storage. Virtually all of the stored compounds were 10−15 years old and were still of high purity and could be used directly for bioassay. These compounds were (**7**−**13**, **16**−**18**, **20**),[46b] (**32**−**39**),[45c] (**40**−**43**, **50**, **51**, **60**−**62**),[46c] (**14**, **21**−**23**, **27**, **29**, **44**−**49**, **52**−**54**, **56**−**59**),[46a] (**63**−**68**),[46d] **69**,[46e] **70**,[46f] (**71**−**72**),[46g] and (**73**, **74**).[46h]

To understand the importance of the peroxide entity for the biological activity in this series, we synthesized a cross section of various 1-deoxoartemisinin derivatives (Scheme 5, **75**−**79**) of the active compounds studied. This was accomplished by hydrogenolysis of an ethyl acetate solution of the corresponding peroxide compounds in the presence of 10% Pd−C. During this process, ring opening of the trioxane ring leads transiently to a tricyclic diol, which readily undergoes loss of water and reketalization to regenerate the noroxatetracycles. Normally, this occurs during the first purification by flash silica gel chromatography. Subsequent rigorous HPLC purification was conducted to ensure that all traces of peroxide were removed.

Scheme 4

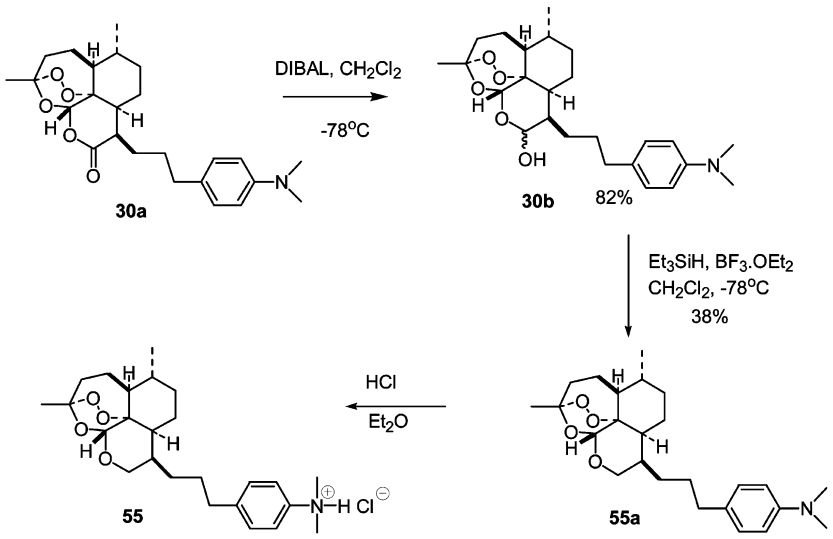

In Vitro Antimalarial and Antileishmania Assay. The antimalarial activity of the analogues was determined in vitro on chloroquine-sensitive (D6-Sierra Leone) and -resistant (W2−Indochina) strains of *P. falciparum*. The 96-well microplate assay is based on evaluation of the effect of the compounds on the growth of asynchronous cultures of *P. falciparum*, determined by the assay of parasite lactate dehydrogenase (pLDH) activity.[47] The appropriate dilutions of the compounds were prepared in DMSO or RPMI-1640 medium and added to the cultures of *P. falciparum* (2% hematocrit, 2% parasitemia) set up in clear flat-bottomed 96-well plates. The plates were placed into the humidified chamber and flushed with a gas mixture of 90% N_2, 5% CO_2, and 5% O_2. The cultures were incubated at 37 °C for 48 h. Growth of the parasite in each well was determined by pLDH assay using Malstat reagent. The medium and RBC controls were also setup in each plate. The standard antimalarial agents, chloroquine and artemisinin, were used as the positive controls while DMSO was tested as the negative control.

Antileishmanial activity of the compounds was tested on a transgenic cell line of *Leishmania donovani* promastigotes expressing firefly luciferase.[48a] In a 96-well microplate assay, compounds with appropriate dilution were added to the leishmania promastigotes culture (2×10^6 cell/mL). The plates were incubated at 26 °C for 72 h and growth of leishmania promastigotes was determined by luciferase assay with Steady Glo reagent (Promega). Pentamidine and amphotericin B were used as standard antileishmanial agents. The analogues were simultaneously tested for cytotoxicity on VERO cells (monkey kidney fibroblast) by Neutral Red assay.[48b]

All the analogues were tested at least at six different concentrations, each in duplicate. The mean values were used to generate the growth inhibition curves and determination of IC_{50} values.

Comparative Molecular Field Analysis (CoMFA). All calculations were carried out on SGI Octane2 machine, equipped with two parallel R12000 processors, V6 graphics board, and 512 MB memory. Sybyl v. 6.9 (Tripos Inc., USA) was utilized for the molecular modeling studies including CoMFA. The CoMFA study was performed on a total of 56 molecules out of 69 listed in Tables 3 and 4. Compounds for which exact IC_{50} values were not available (**28**, **71**, and **74**) were not included in the study. Diastereomeric mixtures and racemates such as the dihydroartemisinin derivatives **40**−**49** were also excluded from the analysis. A test set consisting of 11 molecules with diverse chemical structures and activities was used for validation and was not included in the model development stage. The remaining 45 molecules constituted the training set. The negative logarithm of the molar IC_{50} values (pIC_{50}) was used as activity for the study in order to achieve a normal distribution of activity values.

Using the reported crystal structure for artemisinin[49] as a template, a database of both the test and training set compounds was created. The molecules were minimized with the Tripos force field and aligned by fitting atoms C-1a, C-3, C-5a, and C-8a using the align database command in Sybyl (Figure 1). A similar alignment strategy was successfully used earlier to derive CoMFA models for antimalarial activity of various artemisinin analogues.[45d]

CoMFA involves the measurement of the electrostatic and steric fields around a template molecule and the relationship of these measurements to the molecule's biological activity. These measurements are taken at regular intervals throughout the lattice using a probe atom of designated size and charge. The steric (Lennard-Jones) and electrostatic (Coulomb) interaction energies between a probe atom and the molecules were calculated within a region extending the molecular ensemble by 4 Å in each dimension (x, y, z) with a grid spacing of 2.0 Å. The effect of probe atoms was studied using three different probes: proton, positively charged sp^3 carbon atom, or negatively charged sp^3 oxygen atom. A distance-dependent dielectric constant ($1/r$) was chosen, and the maximum field values were truncated to 30 kcal/mol for the steric and ±30 kcal/mol for the electrostatic interaction energies.

There are numerous formalisms for calculating the partial charges of atoms, and each method has a decisive effect on the overall CoMFA model. To gauge the effect of various charge assignment schemes on the CoMFA results, we calculated partial charges using the Gasteiger−Hückel method,[50] the Gasteiger−Marsili

Table 3. Antileishmanial Activity of Artemisinin Analogues

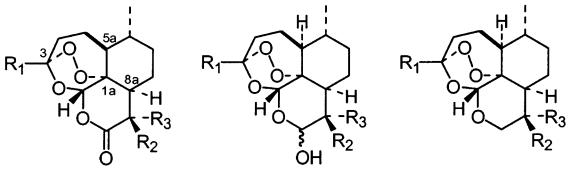

1,7-39 **40-49** **50-62**

no.	R_1	R_2	R_3	IC_{50} (μM)[a]
1	CH_3 (artemisinin)	CH_3	H	124.0
7	CH_3	H	H	242.3
8	CH_3	Et	H	60.7
9	CH_3	CH_3	CH_3	101.2
10	CH_3	^{n}Pr	H	16.8
11	CH_3	$CH_2CH{=}CH_2$	H	17.8
12	CH_3	^{n}Bu	H	12.3
13	CH_3	$(CH_2)_3CH(CH_3)_2$	H	8.5
14	CH_3	$(CH_2)_3CF_3$	H	79.3
15	CH_3	$(CH_2)_2CN$	H	38.9
16	CH_3	CH_2Ph	H	15.3
17	CH_3	$(CH_2)_2Ph$	H	40.3
18	CH_3	$(CH_2)_3Ph$	H	11.6
19	CH_3	H	$(CH_2)_3Ph$	45.3
20	CH_3	$(CH_2)_4Ph$	H	7.5
21	CH_3	$(CH_2)_3C_6H_4$(*m*-F)	H	3.7
22	CH_3	$(CH_2)_3C_6H_4$(*p*-Cl)	H	11.9
23	CH_3	$(CH_2)_3C_6H_4$(*p*-OMe)	H	12.0
24	CH_3	$(CH_2)_3C_6H_4$(*p*-SMe)	H	1.4
25	CH_3	$(CH_2)_3C_6H_4$(*p*-SO_2Me)	H	53.8
26	CH_3	$(CH_2)_3C_6H_4$(*p*-OH)	H	44.7
27	CH_3	$(CH_2)_3C_6H_4(3,5\text{-}(CF_3)_2)$	H	14.4
28	CH_3	H	$(CH_2)_3C_6H_4(3,5\text{-}(CF_3)_2)$	NA[b]
29	CH_3	$(CH_2)_3C_6H_4(3,5\text{-}F_2)$	H	49.7
30	CH_3	$(CH_2)_3C_6H_4$(*p*-NMe_2·HCl)	H	1.9
31	CH_3	H	$(CH_2)_3C_6H_4$(*p*-NMe_2·HCl)	88.3
32	Et	H	H	177.1
33	^{n}Pr	H	H	40.5
34	^{n}Bu	H	H	257.7
35	$(CH_2)_2CO_2Et$	H	H	31.0
36	$(CH_2)_2Ph$	H	H	12.6
37	$(CH_2)_3C_6H_4$(*p*-Cl)	H	H	11.1
38	Et	^{n}Bu	H	35.5
39	$(CH_2)_4Ph$	^{n}Bu	H	4.5
40	CH_3	H	H	44.4
41	CH_3	CH_3	H	70.3
42[c]	CH_3	CH_3	H	44.8
43[d]	CH_3	^{n}Bu	H	382.9
44	CH_3	$(CH_2)_3CF_3$	H	26.3
45[d]	CH_3	$(CH_2)_3C_6H_4$(*p*-CF_3)	H	2.9
46[d]	CH_3	$(CH_2)_3C_6H_4$(*m*-Cl)	H	16.6
47[d]	CH_3	$(CH_2)_3C_6H_4$(*p*-Cl)	H	4.7
48	CH_3	$(CH_2)_3C_6H_4(3,5\text{-}F_2)$	H	33.0
49	CH_3	$(CH_2)_3C_6H_4(3,5\text{-}(CF_3)_2)$	H	NA[b]
50	CH_3	H	H	49.2
51	CH_3	CH_3	H	46.6
52	CH_3	$(CH_2)_3C_6H_4$(*p*-Cl)	H	4.9
53	CH_3	$(CH_2)_3C_6H_4$(*m*-Cl)	H	3.7
54	CH_3	$(CH_2)_3C_6H_4(3,4\text{-}Cl_2)$	H	2.3
55	CH_3	$(CH_2)_3C_6H_4$(*p*-NMe_2·HCl)	H	36.0
56	CH_3	$(CH_2)_3C_6H_4$(*p*-CF_3)	H	1.8
57	CH_3	$(CH_2)_3C_6H_4$(*p*-OMe)	H	17.4
58	CH_3	$(CH_2)_3C_6H_4(3,5\text{-}F_2)$	H	11.0
59	CH_3	$(CH_2)_3C_6H_4(3,5\text{-}(CF_3)_2)$	H	0.3
60	^{n}Pr	H	H	70.8
61	^{n}Bu	H	H	151.8
62	$(CH_2)_2Ph$	H	H	37.7
	amphotericin B			0.01
	pentamidine			1.35

[a] Activity was measured using luciferase assay as described in the text.[48a] Activity for **40**−**49** was measured for the racemic mixture. All the analogues were tested at least at six different concentrations, each in duplicate. The mean values were used to generate the growth inhibition curves and determination of IC_{50} values. [b] Not active up to 125 μg/mL. [c] As arteether. [d] These compounds showed cytotoxicity in the concentration range of 2000−2700 μg/mL while all the other compounds did not exhibit observable cytotoxicity as measured by the procedure described in the text.

Table 4

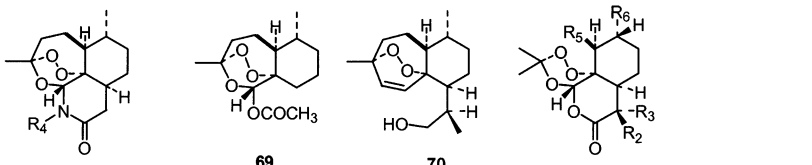

63 R_4 = -$(CH_2)_3CH_3$
64 R_4 = -$(CH_2)^iPr$
65 R4 = -CH_2COO^tBu
66 R4 = -CH_2Ph
67 R4 = -$CH_2C_6H_4$(p-Cl)
68 R4 = -$(CH_2)_2Ph$

69

70

71 R_3=R_5 = H; R_2 = R_6 = CH_3
72 R_3 = H; R_2 = R_5 = R_6 = CH_3
73 R_5 = R_6 = H; R_2 = R_3 = CH_3
74 R_3 = R_5 = R_6 = H, R_2 = CH_2CO_2H

no.	IC_{50} (μM)[a]	no.	IC_{50} (μM)[a]
63	44.5	**69**	148.0
64	185.5	**70**	131.4
65	27.5	**71**	NA[b]
66	56.0	**72**	158.3
67	25.5	**73**	203.5
68	32.3	**74**	NA[b]

[a] Activity was measured using luciferase assay as described in the text.[48a] All the analogues were tested at least at six different concentrations, each in duplicate. The mean values were used to generate the growth inhibition curves and determination of IC_{50} values. [b] Not active up to 125 μg/mL.

Scheme 5

75 R_2 = CH_3; R_3 = H
76 R_2 = $(CH_2)_3C_6H_4$(3,5-diCF_3); R_3 = H
77 R_2 = $(CH_2)_3C_6H_4$(p-SO_2Me); R_3 = H
78 R_2 = $(CH_2)_3C_6H_4$(p-CF_3); R_3 = H
79 R_2 = $(CH_2)_3C_6H_4$(m-Cl); R_3 = H

method,[51] and AM1 calculations using MOPAC 6.0[52] as implemented in Sybyl.

To determine the optimal number of components corresponding to the lowest standard error of prediction and the highest cross-validated r^2 (q^2), SAMPLS[53] with leave-one-out (LOO), no column filtering, and a maximum of 10 variables was carried out. This was followed by cross-validation using the LOO method with the optimal number of components and column filtration values ranging from 0.5 to 2.0 to yield the final q^2 value. The standard CoMFA scaling was applied to both steric and electrostatic energies. The non-cross-validated models were then calculated. Statistical validity of the models was assessed by the variance (r^2), standard error of estimate (S), and the F-values.

The models were further improved by the q^2-guided region selection (q^2-GRS) technique. The q^2-GRS process has been described in detail elsewhere[54] and in recent reviews.[55] Conventional CoMFA routines apply equal weight to data from each lattice point in a given field, whereas the final result actually emphasizes the limited areas of three-dimensional space as important for biological activity. It is suggested that the deficiencies of conventional CoMFA may be overcome by eliminating from the analysis those areas of three-dimensional space where changes in steric and electrostatic field do not

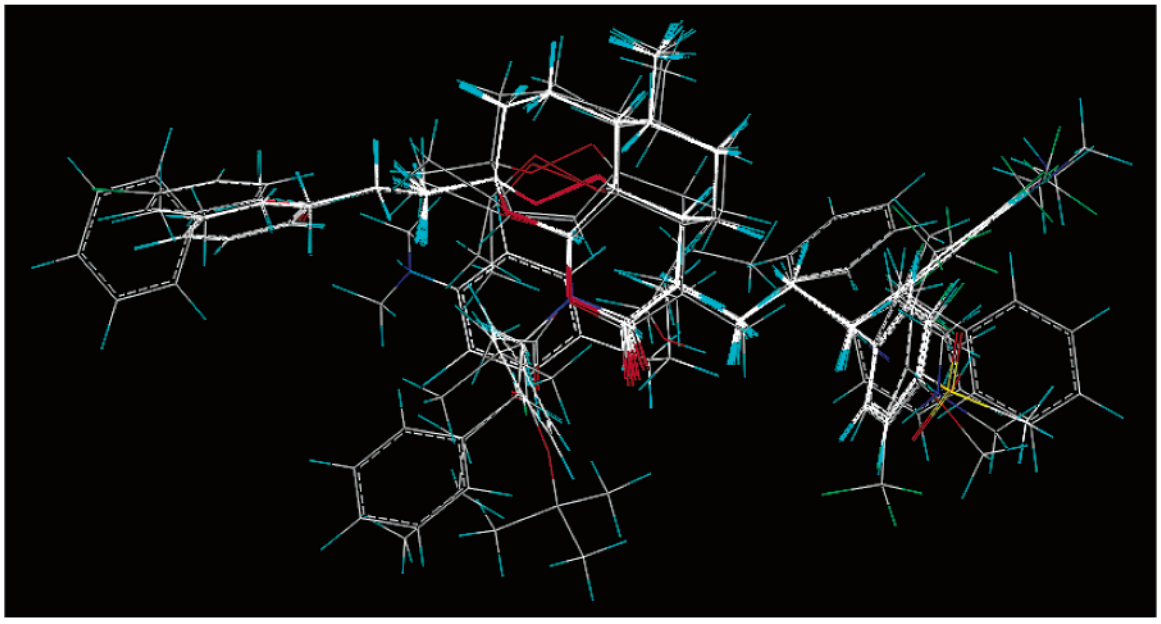

Figure 1. Alignment of artemisinin analogues used for CoMFA model development.

Table 5. Statistical Results of CoMFA Analysis Using q^2-GRS

model	charge[a]	probe[b]	optimum component	CF[c]	q^2	r^2	S	F	r^2_{bs}[d]
1	GH	C.3	6	2.0	0.803	0.966	0.131	179	0.977
2	GH	O.3	6	1.5	0.805	0.969	0.125	196	0.980
3	GH	H	6	1.0	0.774	0.972	0.118	220	0.980
4	GM	C.3	6	0.5	0.712	0.958	0.145	144	0.974
5	GM	O.3	6	1.5	0.732	0.956	0.148	138	0.971
6	GM	H	6	1.5	0.751	0.964	0.134	170	0.975
7	AM1	C.3	4	0.5	0.683	0.964	0.132	264	0.960
8	AM1	O.3	4	0.5	0.670	0.965	0.128	279	0.960
9	AM1	H	4	0.5	0.679	0.956	0.144	218	0.959

[a] GH, Gasteiger−Hückel; GM, Gasteiger−Marsili. [b] H = proton, C.3 = sp^3 carbon with +1 charge, O.3 = sp^3 oxygen with −1 charge. [c] Column filtration value. [d] Mean r^2 values obtained by bootstrap analysis.

correlate with biological activity.[54] The q^2-GRS technique eliminates those areas from the analysis based on low values of q^2 obtained for such regions individually. Thus, it optimizes the region selection for the final PLS analysis. In fact, in the present study, use of the q^2-GRS routine resulted in models with higher q^2 and better statistics.

To cross check for any chance correlations in the PLS analysis, the PLS was repeated with complete randomization of the biological data and the q^2 recalculated. This was repeated 10 times. Also, to obtain statistical confidence limits for the analysis, PLS analysis using 100 bootstrap runs[56] with the optimum number of components was performed.

Models were further evaluated on the basis of their ability to predict activities of the test set molecules. The predictive r^2 for the test set was calculated using the formula, predictive $r^2 = 1 -$ SSD/PRESS, where SSD is the sum of squared deviations from the mean and PRESS is the sum of squared differences between the actual and the predicted values.

Results and Discussion

Antimalarial activities of the new analogues synthesized are presented in Table 2. These compounds were designed and synthesized to improve oral bioavailability and to examine the effect of C-9α/C-9β substitution on the antimalarial activity. The analogues exhibited promising in vitro activity against *P. falciparum* and thus offer an opportunity to develop better artemisinin-based drugs.

To our surprise, most of the artemisinin analogues tested were notably active against leishmania. The activities of these molecules against leishmania are presented in Tables 3 and 4. In general, these can be classified into six different structural classes depending upon the nature and sites of derivatization:[2,45,46] (1) alkyl or arylalkyl groups at the C-3 position, (2) alkyl or arylalkyl groups at C-9, (3) analogues with substitution at both C-3 and C-9 positions, (4) 10-deoxo compounds, (5) lactams, and (6) derivatives that lack one or the other of the artemisinin ring systems (seco ring systems).

An analysis of Table 3 clearly shows that substitution at the C-9β position brings about a significant improvement in the activity compared to artemisinin (**1**). It is more pronounced in the case of phenethyl derivatives with halogens (e.g. **21**, **22** and **27**), SMe (**24**), and NMe_2 (**30**) groups on the aromatic ring. Even though the lactols of this class of compounds were active, the cytotoxicity exhibited by a few of them was discouraging. The 10-deoxo derivatives (**50**−**62**) were expected to be more stable compared to the corresponding acetals, which are relatively unstable due to possible solvolysis or metabolism to a masked aldehyde carbonyl (lactols). The 10-deoxo compounds also exhibited superior activity to the corresponding lactones. The requirement of the unique skeletal framework of artemisinin for its activity is evident from the examples **69**−**74** (Table 4), where one of the rings has been modified. These compounds did not show any noticeable activity against leishmania.

In general, activity against *P. falciparum* appears to be more pronounced (nanomolar range)[45,46] compared to that against *L. donovani* (micromolar range). However, in all the above cases, a similar profile of activity was shown by the artemisinin derivatives against both the organisms. The substitution at C-3 appears to be an exception. Although, bulky substitution at C-3 was shown to improve the antimalarial activity, in case of antileishmanial potency this substitution does not seem to make a significant contribution (Table 3), as exemplified by **34** and **61**. A more quantitative analysis of the structure−activity relationship is presented below.

Structure−Activity Relationship. A comprehensive QSAR study for antimalarial activity of 211 artemisinin analogues (which included most of the molecules presented in this paper) was reported recently by our group[45d] and hence a QSAR study for this activity would be redundant. To determine various factors affecting the antileishmanial activity and understand the relationship between structural requirements for antimalarial vs antileishmanial activity, a CoMFA study was carried out. Several CoMFA models were obtained using different charges, probe atoms, and column filtration values. Statistical results of these models are presented in Table 5.

For any given charge calculation method, the three probes were shown to have little, if any, effect on the overall statistical quality of the models (Table 5). The most significant impact on the model quality was observed with the use of various charge-calculating methods. AM1 charges resulted in models with q^2 values ranging between 0.67 and 0.683. On the other hand, with the use of Gasteiger−Hückel charges q^2 values of more than 0.8 could be obtained. In fact, Gasteiger−Hückel charges are reported to generate reasonable models in various CoMFA studies on artemisinin derivatives.[45d,57,58]

The statistical validity of the models can be judged by high q^2 (more than 0.6) and r^2 (more than 0.9) values along with a low standard error of estimate (less than 0.15). Mean r^2 values for bootstrap analysis of the

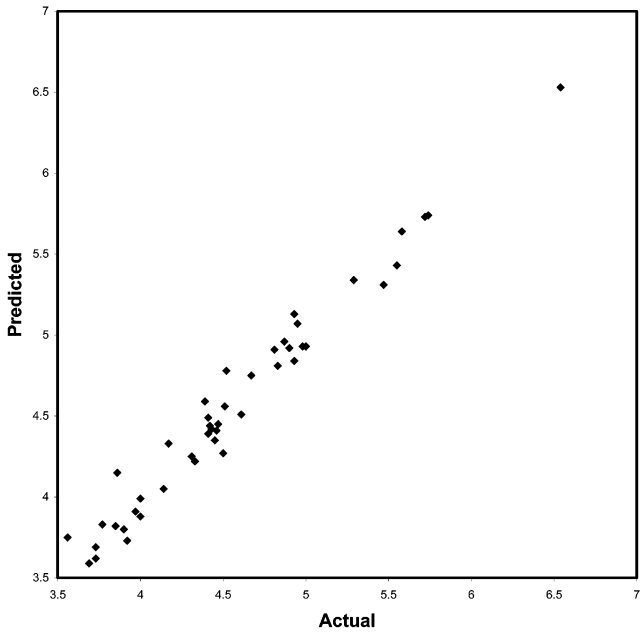

Figure 2. Plot of predicted vs actual activities of compounds in the training set using CoMFA model 2.

Table 6. Residuals for Prediction of Test Set Molecules Using Model 2

molecule	residual (pIC_{50})[a]	molecule	residual (pIC_{50})[a]
14	−0.21	**33**	0.30
19	0.01	**36**	0.31
21	0.24	**50**	0.12
24	0.60	**57**	−0.35
26	−0.13	**58**	−0.32
29	−0.27		

[a] Predictive $r^2 = 0.675$.

models spanned a similar range as that of the r^2 values obtained by non-cross-validated analysis (Table 5). This provided additional validation for the models.

Among the nine statistically significant models, model 2 with the highest q^2 value was utilized for further analysis. The plot of predicted vs actual activity for the training set molecules (Figure 2) reveals an excellent positive correlation between the two activities. To assess the predictive capability of model 2, it was used to predict the activity of a diverse test set of artemisinin derivatives. The result of this prediction is presented in Table 6. The activities predicted by the model are highly consistent with the experimental data. All the residual values for the prediction are less than 1 log order of activity, the highest being 0.60. The mean absolute residual value of 0.44 and the predictive r^2 value of 0.675 suggest the outstanding predictive power of the model.

Model 2 has about 68% contribution from steric field values and 32% from electrostatic field values. The CoMFA contour plots for the steric field are shown in Figure 3 and those for the electrostatic field in Figure 4. The green and yellow areas represent regions where steric bulk is favorable and unfavorable, respectively, for binding. Analogously, red and blue areas represent regions where a negative and a positive charge are favorable, respectively.

The steric map shows a green region (G1, Figure 3) corresponding to the pocket occupied by the C-9β side chain, suggesting that greater steric bulk in this area would increase activity. As an example, **12** with its *n*-butyl side chain at C-9β occupying the G1 region exhibits better leishmanicidal potency compared to artemisinin. However, the presence of a yellow region (Y1, Figure 3) next to the G1 pocket indicates that a longer side chain at C-9β may actually lead to reduction in the activity. Thus, the length of the side chain at the C-9β position appears to be critical for activity. The second yellow region (Y2, Figure 3) is in proximity to the C-10 position, while the third (Y3, Figure 3) is near the C-3 side chain. The presence of Y3 suggests that a bulky group at C-3 would decrease the activity. Although molecules such as **34** and **61**, having a butyl substituent at C-3 and a relatively lower activity, are in agreement with this observation, there are several other molecules such as **36** and **37** that possess higher activity despite having bulky side chains at C-3. Thus, no clear relationship can be derived with respect to the steric effect at the C-3 position. Perhaps, inclusion of more diverse structures at the C-3 position would help to arrive at a more clear relationship.

The important blue and red regions in the electrostatic maps are labeled as B1−B5 and R1−R2, respectively, in Figure 4. Again, most of the contributing regions in terms of electrostatic interactions are related to substitution at the C-9β position. The B1 and B2 regions suggest that a positive charge at the terminal end of a C-9β side chain should improve in vitro activity. This is exemplified by a lower activity of **25** as compared to that of **30**. In the former, a negatively charged sulfonyl group occupies B1 and B2 pockets, which is replaced by positively charged quaternary nitrogen in the latter.

It is interesting to note that 10-deoxo derivatives show improved leishmanicidal activity. For example, compounds such as artemisinin, **22**, **27**, and **34** have a relatively lower potency compared to corresponding 10-deoxo derivatives **51**, **53**, **59**, and **61**, respectively. This may be explained by the presence of B4 close to the C-10 carbonyl oxygen, which indicates that a partial negative charge in this vicinity would lead to a decrease in antileishmanial activity.

The location of R1 and R2 indicates the role of electron-withdrawing groups (negatively charged) on the phenyl ring of the C-9β side chains of the 10-deoxo derivatives. It suggests that negatively charged groups occupying these regions would lead to increased activity. For example, the relative order of activities of **53** < **54** < **56** < **59** may be explained by the observation that the R1 and R2 pockets are occupied by one chloro, two chloro, one CF_3, and two CF_3 groups, respectively, in these molecules. Also, the relatively lower potency of **55** may be attributed to the presence of a quaternary nitrogen on the terminal phenyl ring in proximity to these regions.

It is interesting to compare the results of the current QSAR study of the leishmanicidal activity with that of a comprehensive QSAR study on the antimalarial activity of artemisinin derivatives.[45d] Greater steric bulk near the C-9β side chain was found to improve the antimalarial activity of these derivatives. A similar relationship was observed in the current study on antileishmanial activity. However, in the case of the antimalarial QSAR study, potency was found to have a

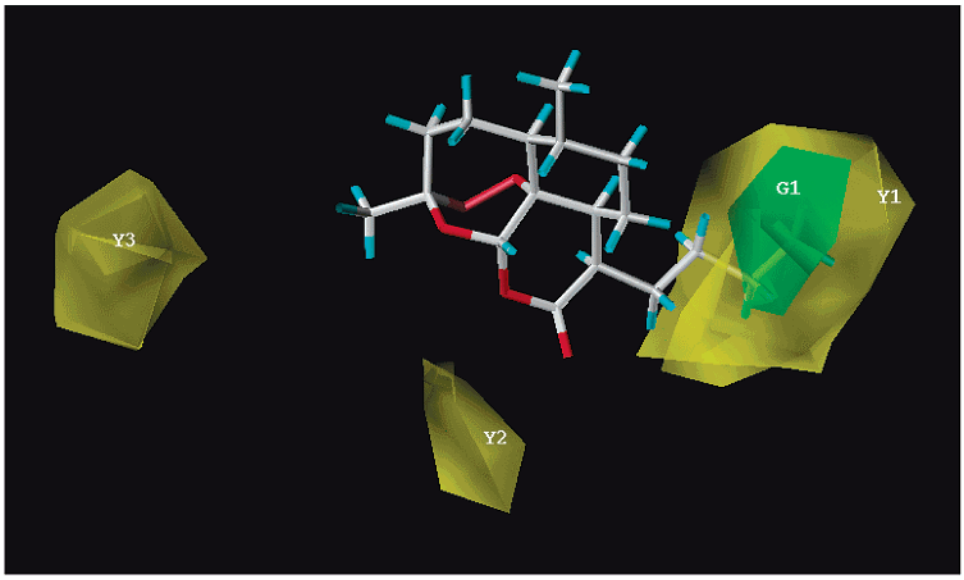

Figure 3. Steric contour map for CoMFA model 2 with **12** as an example. Green contours indicate areas where steric bulk is predicted to increase antileishmanial activity, while yellow contours indicate regions where steric bulk is predicted to decrease activity.

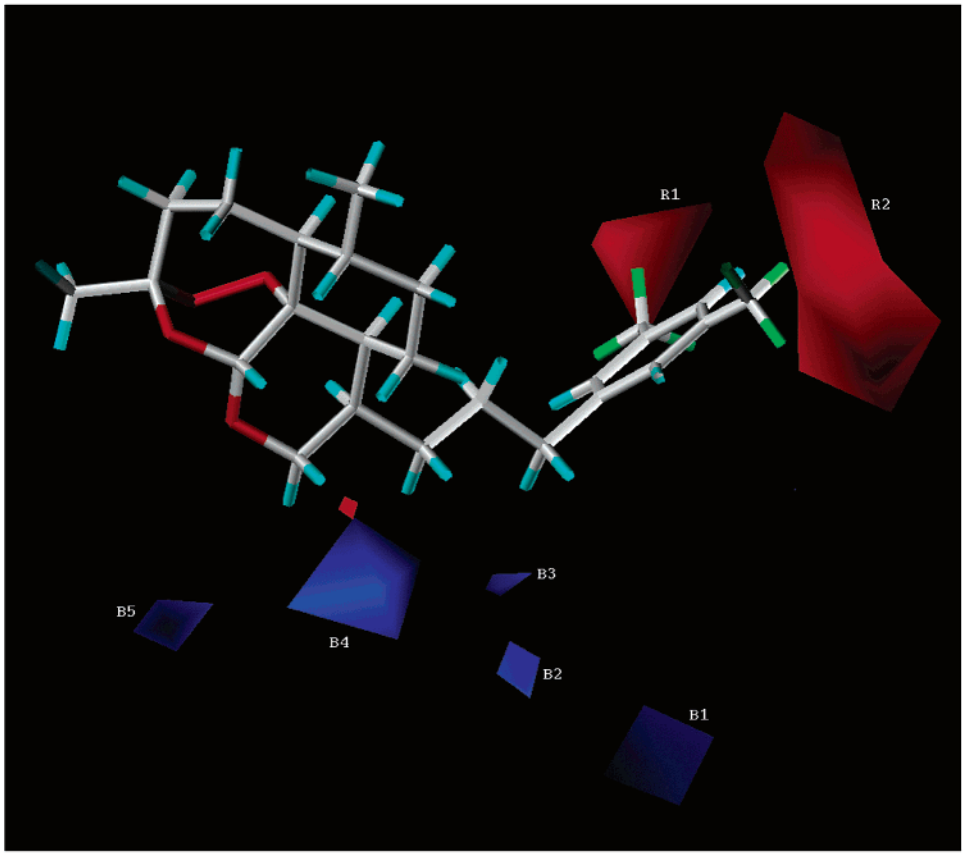

Figure 4. Electrostatic contour map for CoMFA model 2 with **59** as an example. Blue polyhedra indicate regions where partial positive charge is correlated with improved antileishmanial activity, while red polyhedra suggest a relationship between partial negative charge and activity.

positive correlation with increasing steric bulk near the C-3 substituent, whereas no clear relationship was observed between steric bulk at the C-3 position and antileishmanial activity. With respect to the effect of electrostatics on activity, removal of C-10 carbonyl was observed to be favorable for both antimalarial as well as antileishmanial activity.

As was the case for antimalarial activity, the presence of the peroxide moiety appears to be essential for leishmanicidal activity. This is evident from the fact that 1-deoxyartemisinin derivatives **75**−**79** (Scheme 5) do not exhibit leishmanicidal activity. It is also interesting to note the effect of C-9α substitution on both antimalarial and antileishmanial activity. In general,

compounds with C-9α substitution appear to have lower antimalarial (Table 2) as well as antileishmanial activity (Table 3). This is exemplified by compounds **19** and **31**, which show relatively lower potency compared to the corresponding C-9*β*-substituted compounds **18** and **30**, respectively. This could be due to masking of the peroxide group by the substituted aromatic ring when C-9 is in the α orientation. However, it should be noted that the difference in antileishmanial activity between the C-9α− and C-9*β*-substituted compounds is more pronounced than that for antimalarial activity. Compound **28** with C-9α substitution appears to be an exception in this case. While it shows no antileishmanial activity, it has comparable activity to the corresponding C-9*β* derivative **27** against *P. falciparum*.

Possible Mode of Action. As many of the artemisinin derivatives studied were notably leishmanicidal, and the presence of an endoperoxide has been shown to be necessary for antimalarial action,[2] it was logical to study whether the endoperoxide moiety is a key structural feature required for the observed antileishmanial activity. To test this idea, several 1-deoxo derivatives (**75**−**79**) were prepared and tested for their influence on parasitic growth. None of the nonperoxides showed activity in the concentration range tested (up to 125 *μ*g/mL), which clearly emphasizes the role of the peroxide group for the antileishmanial effect.

As described in the Introduction, the mechanism of action of artemisinin against *P. falciparum* is believed to involve free radical intermediates generated in a reaction cascade activated by heme. The leishmania parasite is also known to utilize heme and free iron(II)[59] for its survival, which points toward a potentially similar mode of action.

Finally, it should also be noted that the effect of structural variation on the relative activity appears to be similar for both antimalarial as well as antileishmanial compounds. All these facts together point toward a common mode of action. However, this hypothesis requires further experimental investigation, which is currently being pursued.

Conclusion

Potent antileishmanial activity for a number of artemisinin analogues has been described for the first time. A systematic structure−activity relationship for antileishmanial activity of artemisinin analogues was performed using CoMFA. Substitution at C-9*β* was shown to improve antileishmanial potency compared to artemisinin. This effect was more pronounced with phenethyl substitution. Also, 10-deoxo derivatives exhibited better activity. A similar trend is already known for the antimalarial activity of this class of compounds. The lack of activity in the case of 1-deoxo analogues suggests that the peroxide moiety is required for both antileishmanial as well as antimalarial activity. This in turn points toward a related mode of action for these analogues against *L. donovani* and *P. falciparum*.

Thus, this study suggests the possibility of developing artemisinin analogues as potential drug candidates against both malaria and leishmaniasis. However, considering bioavailability and potential toxicity issues, it would be desirable to bring their antileishmanial activity profile (currently micromolar) at par with that against malaria (nanomolar). Suitable structural modifications based on the results of this study are underway to achieve this goal.

Experimental Section

All reactions were carried out under an argon atmosphere with dry, freshly distilled solvents stored over 4 Å molecular sieves under anhydrous conditions, unless otherwise stated. Thin-layer chromatography (TLC) was performed on precoated silica gel G and GP Uniplates from Analtech. The plates were visualized with a 254 nm UV light, iodine chamber, or charring with acid. Flash chromatography was carried out on silica gel 60 [Scientific Adsorbents Incorporated (SAI), particle size 32−63 *μ*m, pore size 60 Å]. Melting points were noted on a FP62 Mettler Toledo apparatus and are uncorrected. ^{1}H NMR and ^{13}C NMR spectra were recorded on a Bruker DPX 300 operating at 400 and 100 MHz, respectively. The chemical shifts are reported in parts per million (ppm) downfield from tetramethylsilane, and *J* values are in hertz. IR spectra were recorded using a Thermo Nicolet IR 300 FT/IR spectrometer on a germanium crystal plate as neat solids or liquids. Low-resolution mass spectra were recorded using a Waters Micromass ZQ LC-Mass system or Thermo-Finnigan AQA by direct injection in ESI + mode. GC/MS data were obtained with a Hewlett-Packard 5890A gas chromatographic instrument. The high-resolution mass spectra (HRMS) were recorded on a Micromass Q-Tof Micro with lock spray source. Optical rotations were measured on an Autopol IV automatic polarimeter from Rudolph Research Analytical. Elemental analysis data were obtained with a Perkin-Elmer series II 2400 CHNS/O analyzer.

General Procedure for the Preparation of Substituted Phenethyl Alcohols 5a and 5b. To a flame-dried, three-neck, 100 mL round-bottomed flask equipped with a condenser and argon line was added the appropriate carboxylic acid (10 mmol) dissolved in dry THF (25 mL). After cooling to 0 °C, 1 M BH_3·THF (20 mmol) was added dropwise to the stirred mixture and the reaction was then left at 0 °C for 5 h. The reaction mixture was diluted with cold water, washed with a saturated solution of $NaHCO_3$, and extracted with ethyl acetate (3 × 25 mL). The combined organic layers were washed with brine (1 × 25 mL), dried over $MgSO_4$, filtered, and concentrated under reduced pressure. The residue was purified by flash chromatography on silica gel, eluting with 25% ethyl acetate−hexanes to afford the corresponding alcohols.

***p*-(*N*,*N*-Dimethylamino)phenethyl Alcohol (5a).** Yield: 90%. Mp: 56−57 °C. ^{1}H NMR ($CDCl_3$): *δ* 2.77 (t, 2H, *J* = 6.6 Hz), 2.92 (s, 6H, NMe_2), 3.80 (t, 2H, *J* = 6.5 Hz), 6.72 (d, 2H, *J* = 8.53 Hz), 7.10 (d, 2H, *J* = 8.51 Hz). ^{13}C NMR ($CDCl_3$): *δ* 38.21, 40.93 (NMe_2), 64.01, 113.20 (2C, Ar), 126.43 129.72 (2C, Ar), 149.51. IR (neat) cm^{-1}: 3284, 2855, 1617, 1527, 1352, 1049, 1021, 804. HRMS (ESI) *m*/*z*: calcd for $C_{10}H_{15}NO$ [M + H]$^+$ 166.1232, found 166.1225 [M + H]$^+$.

***p*-(Methylthio)phenethyl Alcohol (5b).** Yield: 94%. Mp: 37−38 °C. ^{1}H NMR ($CDCl_3$): *δ* 1.82 (s, 1H), 2.48 (s, 3H), 2.83 (t, 2H, *J* = 6.4 Hz), 3.83 (t, 2H, *J* = 6.8 Hz), 7.16 (d, 2H, *J* = 8.0 Hz), 7.24 (d, 2H, *J* = 8.0 Hz). ^{13}C NMR ($CDCl_3$): *δ* 16.17, 38.62, 63.57, 127.16 (2C, Ar), 129.57 (2C, Ar), 135.57, 136.20. IR (neat) cm^{-1}: 3408, 2949, 1495, 1429, 1037, 1021, 808 cm^{-1}. GCMS (EI) *m*/*z*: calcd for $C_9H_{12}OS$ (M$^+$, 168), found 168 [M$^+$].

Triisopropyl Silyl Ether Protection of 4-Hydroxyphenylacetic Acid Methyl Ester (4c). To an ice-cooled, stirred solution of the phenolic ester **4c** (5.0 g, 30 mmol) and imidazole (2.4 g, 35.25 mmol) in dry DMF (20 mL) in a dried round-bottomed flask was added dropwise triisopropylsilyl chloride (6.6 mL, 30.8 mmol), and the solution was stirred for 5 h, slowly warming to room temperature. The mixture was then washed with water (1 × 25 mL) and extracted with ether (3 × 30 mL). The combined organic layers were washed with brine (1 × 25 mL), dried over $MgSO_4$, and filtered. The solvents were evaporated under reduced pressure. The crude product was purified by flash chromatography over silica gel, eluting with 5% ethyl acetate−hexanes to afford 9.5 g of the product **4c′** as an oily liquid. Yield: 98%. ^{1}H NMR ($CDCl_3$): *δ* 1.13 (d,

18H, J = 7.2 Hz), 1.28 (m, 3H), 3.54 (s, 2H), 3.70 (s, 3H), 6.85 (d, 2H, J = 8.4 Hz), 7.15 (d, 2H, J = 8.4 Hz). ^{13}C NMR ($CDCl_3$): δ 12.68, 17.91, 40.36, 51.90, 119.89, 126.34, 130.17, 155.17, 172.35. IR (neat) cm^{-1}: 2945, 2868, 1740, 1511, 1266, 1156, 915, 686. GCMS (EI) m/z: calcd for $C_{18}H_{30}O_3Si$ (M^+), found 322 [M^+].

Preparation of 4-(Triisopropylsilyloxy)phenylethyl Alcohol (5c). To an ice-cooled, stirred suspension of lithium aluminum hydride (0.37 g, 9.6 mmol) in dry ether (12 mL) in 50 mL round-bottom flask was added dropwise a solution of **4c′** (1.55 g, 4.8 mmol) in ether (15 mL), and the mixture was stirred for 1 h, the reaction being monitored by TLC until completion. A saturated solution of sodium sulfate (10 mL) was added to this dropwise at 0 °C. The solids were filtered and washed with ether (3 × 30 mL). The organic layers were combined, dried over $MgSO_4$, and filtered. The combined solvents were removed in vacuo. The residue was purified by flash chromatography on a silica gel column using 15% ethyl acetate−hexanes to afford 1.1 g of **5c** as an oily liquid. Yield: 83%. ^{1}H NMR ($CDCl_3$): δ 1.1 (d, 18H, J = 7.0 Hz), 1.25 (m, 3H), 2.79 (t, 2H, J = 6.6 Hz), 3.81 (t, 2H, J = 6.62 Hz), 6.82 (d, 2H, J = 8.35 Hz), 7.05 (d, 2H, J = 8.34 Hz). ^{13}C NMR ($CDCl_3$): δ 12.69, 17.94, 38.40, 63.80, 119.94 (2C, Ar), 129.88 (2C, Ar), 130.71, 154.67. IR (neat) cm^{-1}: 3330, 2953, 2868, 1605, 1511, 1266, 1046, 914. GCMS (m/z): calcd for $C_{17}H_{30}O_2Si$ (M^+, 294), found 294 [M^+].

Preparation of *p*-(*N*,*N*-Dimethylamino)phenethyl Bromide (6a). To a dried 10 mL round-bottomed flash under argon at 0 °C was added **5a** (0.1 g, 0.6 mmol), CH_2Cl_2 (2 mL), and carbon tetrabromide (0.3 g, 0.9 mmol), followed by dropwise addition of a solution of triphenylphosphine (0.16 g, 0.6 mmol) in dry CH_2Cl_2 (1 mL). The mixture was warmed to room temperature after 2 h, the reaction being monitored by TLC for completion. The reaction mixture was then washed with water (1 × 10 mL), and the aqueous layer was extracted with CH_2Cl_2 (2 × 5 mL). The combined organic layers were dried over $MgSO_4$ and filtered. The solvents were evaporated under reduced pressure. The residue was purified by flash chromatography on silica gel (∼20 g), eluting with hexanes to afford 0.86 g of **6a**. Yield: 63%. Mp: 45−46 °C. ^{1}H NMR ($CDCl_3$): δ 2.93 (s, 6H), 3.07 (t, 2H, J = 7.92 Hz), 3.51 (t, 2H, J = 7.7 Hz), 6.70 (d, 2H, J = 8.56 Hz), 7.09 (d, 2H, J = 8.50 Hz). ^{13}C NMR ($CDCl_3$): δ 33.83, 38.74, 40.75 (NMe_2), 112.82 (2C, Ar), 126.87, 129.41 (2C, Ar), 149.67. IR (neat) cm^{-1}: 2900, 1613, 1519, 1352, 1204, 808. HRMS (ESI) m/z: calcd for $C_{10}H_{14}BrN$ [M + H]$^+$ 228.0388, found 228.0380 [M + H]$^+$.

Preparation *p*-(Methylthio)phenethyl Bromide (6b) and 4-(Triisopropylsilyloxy)phenethyl Bromide (6c). In a dried 25 mL round-bottomed flask under argon was taken a solution of the appropriate alcohol (1 mmol) in ether/acetonitrile (3:1, 10 mL). Triphenylphosphine (3 equiv) was added to this solution, followed by imidazole (3 equiv) and then bromine (3 equiv), and the mixture was stirred at room temperature for 2 h, the progress being monitored by TLC. The reaction mixture was filtered and washed with ether (2 × 15 mL). The organic layers were combined, washed with brine (1 × 25 mL), dried over $MgSO_4$, and filtered. The combined solvents were evaporated under reduced pressure. The residue was purified by flash chromatography on silica gel, eluting with 1% ethyl acetate−hexanes to afford the corresponding bromides.

6b. Yield: 92%. ^{1}H NMR ($CDCl_3$): δ 2.48 (s, 3H), 3.12 (t, 2H, J = 7.6 Hz), 3.54 (t, 2H, J = 7.6 Hz), 7.14 (d, 2H, J = 8.11 Hz), 7.22 (d, 2H, J = 8.12 Hz). ^{13}C NMR ($CDCl_3$): δ 16.42, 33.47, 39.25, 127.35 (2C, Ar), 129.62 (2C, Ar), 136.18, 137.40. IR (neat) cm^{-1}: 2921, 1495, 1437, 1095, 809. GCMS (EI) m/z: calcd for $C_9H_{11}BrS$ (M^+, 230), found 230 [M^+].

6c. Yield: 75%. ^{1}H NMR ($CDCl_3$): δ 1.12 (d, 18H, J = 7.6 Hz), 1.27 (m, 3H), 3.09 (t, 2H, J = 8.0 Hz), 3.53 (t, 2H, J = 7.6 Hz), 6.84 (d, 2H, J = 8.40 Hz), 7.06 (d, 2H, J = 8.40 Hz). ^{13}C NMR ($CDCl_3$): δ 12.69 (3C, CHs), 17.95 (6 × CH_3), 33.28, 38.82, 119.99 (2C, Ar), 129.58 (2C, Ar), 131.40, 155.02. IR (neat) cm^{-1}: 2946, 2864, 1736, 1511, 1266, 914. GCMS (EI) m/z: calcd for $C_{17}H_{29}BrOSi$ (M^+, 356), found 356 [M^+].

General Procedure for the Radical-Induced Michael Addition of Various Aryl Alkyl or Alkyl Bromides to Artemisitene. To a stirred solution of artemisitene[46a] (1 mmol) in dry benzene (30 mL) in a two-necked 100 mL round-bottom flask equipped with a condenser and an argon line was added a bromide derivative (**6a**−**6d**, 1.3 mmol) and AIBN (0.1 mmol). The reaction mixture was heated to reflux, and a solution of tributyltin hydride (1.4 mmol) in benzene (20 mL) was added to it via a syringe pump over a period of 8 h. After the addition was completed, the reaction mixture was refluxed for another 1 h. The flask was then cooled to room temperature, and the solvent was evaporated under reduced pressure. The residue was diluted with ether (15 mL), and a saturated solution of potassium fluoride (5 mL) was added. The mixture was stirred at room temperature for 12 h and filtered and the filtrate washed with water. The organic layer was dried over anhydrous $MgSO_4$ and filtered, and the combined solvents were evaporated under reduced pressure to give a crude residue, which was purified by flash column chromatography on silica gel using 15% ethyl acetate−hexanes to afford the α- and β-isomers. The α-isomer could be converted to the β-form by refluxing with DBU in THF for 12 h.

(+)-Octahydro-3,6α-dimethyl-3,12-epoxy-9β-(2′-cyanoethyl)-12*H*-pyrano[4,3*j*]-1,2-benzodioxepin-10(3*H*)-one (15). Yield: 14%. Mp: 171−172 °C. $[\alpha]^{24}_D$ +120.0 ($CHCl_3$, c 0.5). ^{1}H NMR ($CDCl_3$): δ 1.0 (d, 3H, J = 5.55 Hz), 1.12 (m, 2H), 1.42 (m, 3H), 1.45 (s, 3H), 1.61−1.64 (m, 2H), 1.79−1.88 (m, 2H), 2.01−2.10 (m, 2H), 2.20−3.30 (m, 1H), 2.40−2.48 (m, 1H), 2.57−2.63 (m, 1H), 2.77−2.85 (m, 1H), 3.30 (m, 1H), 5.87 (s, 1H). ^{13}C NMR ($CDCl_3$): δ 16.37, 19.76, 23.60, 24.58, 24.78, 25.12, 33.35, 35.81, 37.38, 37.45, 44.36, 49.89, 79.05, 93.87, 105.60, 119.27, 170.64. IR (neat) cm^{-1}: 2933, 2864, 1732, 1442, 1384, 1115, 984. HRMS (ESI) m/z: calcd for $C_{17}H_{23}NO_5Na$ [M + Na]$^+$ 344.1474, found 344.1492 [M + Na]$^+$. Anal. ($C_{17}H_{23}NO_5$): C, H.

(+)-Octahydro-3,6α-dimethyl-3,12-epoxy-9α-(3′-phenylpropyl)-12*H*-pyrano[4,3*j*]-1,2-benzodioxepin-10(3*H*)-one (19). This analogue was prepared by radical-induced Michael addition of phenethyl iodide to artemisitene according to the general procedure described above. Yield: 30%. $[\alpha]^{26}_D$ +92.0 ($CHCl_3$, c 0.5). ^{1}H NMR ($CDCl_3$): δ 0.98 (d, 3H, J = 5.64 Hz), 1.01 (m, 1H), 1.40 (m, 4H), 1.45 (s, 3H), 1.75 (m, 6H), 2.08 (m, 4H), 2.40 (m, 1H), 2.62 (t, 2H, J = 7.3 Hz), 5.90 (s, 1H), 7.17−7.29 (m, 5H). ^{13}C NMR ($CDCl_3$): δ 19.91, 24.75, 25.50, 29.70, 31.66, 34.02, 34.12, 35.87, 35.95, 37.57, 42.81, 45.06, 50.54, 80.31, 93.73, 105.29, 125.81, 128.36 (2C, Ar), 128.41 (2C, Ar), 142.22, 171.88. IR (neat) cm^{-1}: 2929, 2851, 1740, 1458, 1380, 1106, 996. HRMS (ESI) m/z: calcd for $C_{23}H_{30}O_5Na$ [M + Na]$^+$ 409.1991, found 409.1978 [M + Na]$^+$. Anal. ($C_{23}H_{30}O_5 \cdot H_2O$): C, 68.64; H, 7.92.

(+)-Octahydro-3,6α-dimethyl-3,12-epoxy-9β-(3′-(*p*-methylthiophenyl)propyl)-12*H*-pyrano[4,3*j*]-1,2-benzodioxepin-10(3*H*)-one (24). Yield: 17%. Mp: 164−165 °C. $[\alpha]^{25}_D$ +54.0 ($CHCl_3$, c 0.5). ^{1}H NMR ($CDCl_3$): δ 0.99 (d, 3H, J = 5.8 Hz), 1.04 (m, 2H), 1.38 (m, 3H), 1.44 (s, 3H), 1.56 (m, 3H), 1.74 (m, 3H), 2.05 (m, 3H), 2.41 (m, 1H), 2.46 (s, 3H), 2.57 (m, 1H), 2.63 (m, 1H), 3.21 (m, 1H), 5.83 (s, 1H), 7.10 (d, 2H, J = 8.10 Hz), 7.20 (d, 2H, J = 8.11 Hz). ^{13}C NMR ($CDCl_3$): δ 16.69, 20.22, 23.66, 25.26, 25.58, 26.62, 29.20, 33.97, 35.52, 36.32, 37.89, 38.07, 43.27, 50.46, 79.60, 93.82, 105.74, 127.52 (2C, Ar), 129.33 (2C, Ar), 135.73, 139.44, 171.80. IR (neat) cm^{-1}: 2926, 2866, 1739, 1189, 1109, 1000. ESI MS m/z: calcd for $C_{24}H_{32}O_5S$ [M + H]$^+$ 433.2048, found 433.3 [M + H]$^+$, 865.4 [2M + H]$^+$, 887.4 [2M + Na]$^+$. Anal. ($C_{24}H_{32}O_5S \cdot 0.5H_2O$): C, H.

(+)-Octahydro-3,6α-dimethyl-3,12-epoxy-9β-(3′-(*p*-triisopropylsilyloxyphenyl)propyl)-12*H*-pyrano[4,3*j*]-1,2-benzodioxepin-10(3*H*)-one (26b). Yield: 22%. $[\alpha]^{25}_D$ +84.0 ($CHCl_3$, c 0.5). ^{1}H NMR ($CDCl_3$): δ 0.98 (d, 3H, J = 5.27 Hz), 1.02 (m, 2H), 1.08 (d, 18H, J = 6.98 Hz), 1.22 (m, 6H), 1.38 (s, 3H), 1.70 (m, 6H), 2.04 (m, 3H), 2.50 (m, 3H), 3.21 (m, 1H), 5.82 (s, 1H), 6.77 (d, 2H, J = 8.17 Hz), 7.0 (d, 2H, J = 8.23 Hz). ^{13}C NMR ($CDCl_3$): δ 13.02 (3 × CH), 18.33 (6 × CH_3), 20.20, 23.58, 25.25, 25.55, 26.49, 29.37, 33.97, 35.23, 36.31,

37.88, 38.04, 43.13, 50.46, 79.58, 93.77, 105.68, 120.06 (2C, Ar), 129.53 (2C, Ar), 134.70, 154.43, 171.81. IR (neat) cm^{-1}: 2917, 2860, 1736, 1515, 1462, 1266, 1101, 1001, 914, 882, 681. ESI MS *m/z*: calcd For $C_{32}H_{50}O_6Si$ $[M + H]^+$ 559.3455, found 559.5 $[M + H]^+$, 1116.9 $[2M + H]^+$.

(+)-Octahydro-3,6α-dimethyl-3,12-epoxy-9α-(3′-(3,5-bis-(trifluoromethyl)phenyl)propyl)-12*H*-pyrano[4,3*j*]-1,2-benzodioxepin-10(3*H*)-one (28). This analogue was synthesized as reported previously.[46a] Yield: 43%. $[\alpha]^{26}_D$ +92.0 ($CHCl_3$, *c* 0.5). ^1H NMR ($CDCl_3$): δ 1.0 (d, 3H, $J = 5.6$ Hz), 1.13 (m, 1H), 1.46 (s, 3H), 1.47−1.52 (m, 4H), 1.74 (m, 3H), 1.83 (m, 3H), 1.98 (m, 1H), 2.05−2.18 (m, 3H), 2.39 (m 1H), 2.78 (t, 2H, $J = 7.6$ Hz), 5.92 (s, 1H), 7.65 (s, 2H), 7.71 (s, 1H). ^{13}C NMR ($CDCl_3$): δ 19.83, 24.70, 25.40, 29.13, 31.57, 33.86, 33.95, 35.52, 35.90, 37.52, 43.12, 44.95, 50.51, 80.13, 93.80, 105.33, 119.96, 122.08, 124.79, 128.57, 131.37, 131.70, 144.51 (2C), 171.51. IR (neat) cm^{-1}: 2925, 2868, 1740, 1381, 1279, 1168, 1136, 1001, 890. HRMS (ESI) *m/z*: calcd for $C_{25}H_{28}F_6O_5$-Na $[M + Na]^+$ 545.1739, found 545.1740 $[M + Na]^+$, 561.1382 $[M + K]^+$. Anal. ($C_{25}H_{28}F_6O_5$): C, H.

(+)-Octahydro-3,6α-dimethyl-3,12-epoxy-9*β*-(3′-(*p*-*N*,*N*-dimethylaminophenyl)propyl)-12*H*-pyrano[4,3*j*]-1,2-benzodioxepin-10(3*H*)-one (30a). Yield: 30%. Mp: 167−169 °C. $[\alpha]^{26}_D$ +68.0 ($CHCl_3$, *c* 1.0). ^1H NMR ($CDCl_3$): δ 0.98 (d, 3H, $J = 5.73$ Hz), 1.03 (m, 1H), 1.38 (m, 4H), 1.44 (s, 3H), 1.59−1.80 (m, 6H), 2.01−2.20 (m, 3H), 2.41−2.70 (m, 3H), 2.90 (s, 6H), 3.21 (ddd, 1H, $J = 5.33$, 1.7, 5.2 Hz), 5.83 (s, 1H), 6.69 (d, 2H, $J = 8.61$ Hz), 7.05 (d, 2H, $J = 8.52$ Hz). ^{13}C NMR ($CDCl_3$): δ 20.23, 23.65, 25.29, 25.59, 26.52, 29.44, 34.03, 35.02, 36.35, 37.96, 38.05, 41.32 (2C), 43.10, 50.54, 79.62, 93.80, 105.74, 113.45 (2C, Ar), 129.32 (2C, Ar), 130.58, 149.51, 171.93. IR (neat) cm^{-1}: 2921, 1748, 1613, 1523, 1180, 1119, 1033, 996, 804. HRMS (ESI) *m/z*: calcd for $C_{25}H_{35}NO_5$ $[M + H]^+$ 430.2593, found 430.2587 $[M + H]^+$, 452.2424 $[M + Na]^+$. Anal. ($C_{25}H_{35}$-NO_5): C, H, N.

30 (Hydrochloride salt of **30a**). ^1H NMR ($CDCl_3$): δ 0.98 (d, 3H, $J = 5.52$ Hz), 1.04 (m, 1H), 1.36 (m, 2H), 1.42 (s, 3H), 1.70 (m, 1H), 1.75 (m, 6H), 1.98 (m, 4H), 2.40 (m, 1H), 2.67 (m, 2H), 3.14 (s, 6H), 3.18 (m, 1H), 5.83 (s, 1H), 7.29 (d, 2H, $J = 8.16$ Hz), 7.64 (d, 2H, $J = 8.04$ Hz). IR (neat) cm^{-1}: 2933, 1736, 1519, 1454, 1376, 1196, 1119, 1037, 1000.

(+)-Octahydro-3,6α-dimethyl-3,12-epoxy-9α-(3′-(*p*-*N*,*N*-dimethylaminophenyl)propyl)-12*H*-pyrano[4,3*j*]-1,2-benzodioxepin-10(3*H*)-one (31). Yield: 32%. Mp: 145−147 °C. $[\alpha]^{26}_D$ +88.0 ($CHCl_3$, *c* 0.5). ^1H NMR ($CDCl_3$): δ 0.98 (d, 3H, $J = 5.76$ Hz), 1.37−1.44 (m, 4H), 1.45 (s, 3H), 1.64−1.77 (m, 7H), 2.04−2.13 (m, 4H), 2.37 (m, 1H), 2.53 (m, 2H), 2.90 (s, 6H), 5.89 (s, 1H), 6.69 (d, 2H, $J = 8.64$ Hz), 7.06 (d, 2H, $J = 8.55$ Hz). ^{13}C NMR ($CDCl_3$): δ 19.96, 24.76, 25.54, 30.12, 31.66, 34.0, 34.12, 34.84, 35.95, 37.56, 40.99 (NMe_2), 42.63, 45.06, 50.51, 80.39, 93.72, 105.27, 113.07 (2C, Ar), 128.98 (2C, Ar), 130.51, 149.06, 172.05. IR (neat) cm^{-1}: 2917, 2851, 1732, 1621, 1523, 1343, 1209, 1168, 1102. LCMS (ESI) *m/z*: calcd for $C_{25}H_{35}NO_5$ $[M + H]^+$ 430, found 430 $[M + H]^+$, 447 $[M + NH_4]^+$. Anal. ($C_{25}H_{35}NO_5$·EtOAc): C, 66.65; H, 8.20; N, 2.70.

(+)-Octahydro-3,6α-dimethyl-3,12-epoxy-9*β*-(3′-(*p*-methanesulfonylphenyl)propyl)-12*H*-pyrano[4,3*j*]-1,2-benzodioxepin-10(3*H*)-one (25). To a stirred solution of **24** (0.42 g, 0.96 mmol) in dry CH_2Cl_2 (40 mL) at −78 °C was added a solution of *m*-CPBA (0.49 g, 77%, 2.2 mmol) in CH_2Cl_2 (40 mL) over a period of 2.5 h. The reaction mixture was stirred at that temperature for another 1.5 h. To this mixture was added water (10 mL), followed by solid $NaHCO_3$ (7.0 g). The reaction mixture was allowed to warm to room temperature, and the product was extracted with CH_2Cl_2 (3 × 30 mL). The combined organic layers were washed sequentially with 7% $NaHCO_3$ solution, water (1 × 25 mL), brine (1 × 25 mL), and dried over anhydrous Na_2SO_4. The solvents were removed under reduced pressure to afford the crude product, which was purified by flash column chromatography on silica gel using 3−4% EtOAc−CH_2Cl_2 as the eluent to yield 0.42 g of **25**. Yield: 94%. Mp: 157−158 °C. $[\alpha]^{25}_D$ +59.0 ($CHCl_3$, *c* 1.0). ^1H NMR ($CDCl_3$): δ 0.99 (d, 3H, $J = 5.46$ Hz), 1.08 (m, 2H), 1.30 (m, 4H), 1.39 (s, 3H), 1.57 (d, 1H, $J = 4.7$ Hz), 1.74 (m, 4H), 2.02 (m, 3H), 2.41 (m, 1H), 2.75 (m, 2H), 3.04 (s, 3H), 3.21 (m, 1H), 5.83 (s, 1H), 7.37 (d, 2H, $J = 8.07$ Hz), 7.84 (d, 2H, $J = 8.03$ Hz). ^{13}C NMR ($CDCl_3$): δ 14.47, 20.13, 22.96, 23.65, 25.16, 25.50, 26.78, 28.90, 31.90, 33.86, 35.98, 36.24, 37.78, 38.07, 43.46, 44.90, 50.37, 79.57, 93.85, 105.70, 127.82 (2C, Ar), 129.70 (2C, Ar), 138.54, 148.91, 171.66. IR (KBr) cm^{-1}: 3017, 2926, 2869, 1735, 1302, 1191, 1146, 1110, 998. ESI MS *m/z*: calcd for $C_{24}H_{32}O_7S$ $[M + H]^+$ 465.1947, found 465.2 $[M + H]^+$, 929.3 $[2M + H]^+$, 951.3 $[2M + Na]^+$. Anal. ($C_{24}H_{32}O_7S$): C, H.

(+)-Octahydro-3,6α-dimethyl-3,12-epoxy-9*β*-(3′-(*p*-hydroxyphenyl)propyl)-12*H*-pyrano[4,3*j*]-1,2-benzodioxepin-10(3*H*)-one (26). To a stirred solution of **26b** (0.76 g, 1.36 mmol) in dry THF (12 mL) was added tetrabutylammonium fluoride (0.34 mL, 1.0 M solution in THF) dropwise and the mixture was stirred at room temperature for 2 h, the progress of the reaction being monitored by TLC. The solvent was evaporated under reduced pressure, and the residue was purified by flash column chromatography on silica gel using 15% EtOAc−hexanes as the eluent to afford 0.5 g of **26**. Yield: 91%. Mp: 116−117 °C. $[\alpha]^{25}_D$ +78.0 ($CHCl_3$, *c* 1.0). ^1H NMR ($CDCl_3$): δ 0.98 (d, 3H, $J = 5.56$ Hz), 1.03 (m, 2H), 1.34 (m, 4H), 1.43 (s, 3H), 1.45−1.79 (m, 6H), 2.05 (m, 3H), 2.40−2.70 (m, 3H), 3.21 (m, 1H), 5.83 (s, 1H), 6.74 (d, 2H, $J = 8.42$ Hz), 7.03 (d, 2H, $J = 8.31$ Hz). ^{13}C NMR ($CDCl_3$): δ 20.19, 23.64, 25.24, 25.54, 26.51, 29.46, 33.94, 35.16, 36.31, 37.89, 38.14, 43.12, 50.43, 79.68, 94.03, 105.86, 115.74 (2C, Ar), 129.70 (2C, Ar), 133.92, 154.57, 172.60. IR (KBr) cm^{-1}: 3386, 2928, 2872, 1733, 1715, 1613, 1514, 1445, 1378, 1202, 1113, 1000. ESI MS (*m/z*) calcd for $C_{23}H_{30}O_6$ $[M + H]^+$ 403.2, found 403.2 $[M + H]^+$, 805.6 $[2M + H]^+$, 827.5 $[2M + Na]^+$. Anal. ($C_{23}H_{30}O_6$·$0.5H_2O$): C, H.

(+)-Octahydro-3,6α-dimethyl-3,12-epoxy-9*β*-(3′-(*p*-*N*,*N*-dimethylaminophenyl)propyl)-12*H*-pyrano[4,3*j*]-1,2-benzodioxepin (55a). To a stirred solution of **30a** (0.41 g, 0.953 mmol) in dry CH_2Cl_2 (5 mL) at −78 °C was added 1 M diisobutylaluminum hydride in CH_2Cl_2 (1.1 mL, 1.1 equiv), and the reaction mixture was stirred for 2 h. It was then quenched with saturated $NaHCO_3$ (5 mL), diluted with CH_2Cl_2 (10 mL), and allowed to warm to room temperature. The mixture was then washed with 10% HCl/saturated NH_4Cl (1:15 v/ v). The organic layer was dried over Na_2SO_4 and filtered, and the combined organic solvents were concentrated under reduced pressure to afford a residue, which was chromatographed on a short silica gel column using CH_2Cl_2−EtOAc (3:1) solvent system to yield 0.333 g (82%) of the lactol as an isomeric mixture, which was used for the next reduction.

To a stirred solution of the lactol (**30b**) (0.33 g, 0.77 mmol) in dry CH_2Cl_2 (6 mL) at −78 °C was added triethylsilane (0.49 mL, 3.06 mmol) and the mixture stirred for 10 min. To this was added BF_3·OEt_2 (0.5 mL, 1.15 mmol) and the mixture stirred at that temperature for 7 h. It was then quenched with pyridine and allowed to warm to room temperature. This mixture was then poured into aqueous saturated NH_4Cl (10 mL) and extracted with EtOAc (3 × 25 mL). The combined organic layers were dried over anhydrous Na_2SO_4 and filtered. The solvents were evaporated in vacuo. The residue was chromatographed over silica gel using 15% EtOAc−hexanes to afford 0.11 g of **55a**. Yield: 35%. Mp: 131−132 °C. $[\alpha]^{26}_D$ +78.0 ($CHCl_3$, *c* 0.5). ^1H NMR ($CDCl_3$): δ 0.95 (d, 3H, $J = 6.13$ Hz), 0.96−1.40 (m, 4H), 1.42 (s, 3H), 1.44−1.74 (m, 8H), 1.80−1.95 (m, 1H), 1.96−2.10 (m, 1H), 2.30−2.60(m, 4H), 2.91 (s, 6H), 3.42 (dd, 1H, $J = 11.69$, 11.70 Hz), 3.79 (dd, 1H, $J = 3.78$, 3.95 Hz), 5.19 (s, 1H), 6.68 (d, 2H, $J = 8.53$ Hz), 7.03 (d, 2H, $J = 8.52$ Hz). ^{13}C NMR ($CDCl_3$): δ 20.71, 21.31, 25.16, 26.52, 27.63, 29.02, 33.34, 34.47, 35.25, 36.66, 37.74, 41.33 (2C, NMe_2), 43.67, 52.65, 65.66, 81.10, 92.82, 104.56, 113.40 (2C, Ar), 129.30 (2C, Ar), 130.78, 150.0. IR (neat) cm^{-1}: 2933, 1621, 1523, 1454, 1348, 1135, 1098, 1061, 874, 808. HRMS (ESI) *m/z*: calcd for $C_{25}H_{37}NO_4$ $[M + H]^+$ 416.2801, found 416.2812 $[M + H]^+$, 438.2639 $[M + Na]^+$. Anal. ($C_{25}H_{37}NO_4$): C, H, N.

55 (hydrochloride). ^1H NMR ($CDCl_3$): δ 0.89 (d, 3H, $J = 6.12$ Hz), 0.98−1.29 (m, 3H), 1.35 (s, 3H), 1.38−1.66 (m, 9H), 1.80 (m, 1H), 1.84−1.97 (m, 1H), 2.27 (dd, 1H, $J = 3.20$, 3.70 Hz), 2.38 (m, 1H), 2.55 (t, 2H, $J = 7.23$ Hz), 3.12 (s, 6H), 3.39

(dd, 1H, J = 5.83, 11.64 Hz), 3.70 (dd, 1H, J = 3.48, 3.57 Hz), 5.13 (s, 1H), 7.22 (d, 2H, J = 7.7 Hz), 7.63 (d, 2H, J = 7.86 Hz). ^{13}C NMR ($CDCl_3$): δ 20.65, 21.28, 25.05, 26.44, 27.50, 28.56, 33.26, 34.33, 35.69, 36.58, 37.64, 43.70, 47.03, 52.55, 53.88, 65.34, 81.00, 92.71, 104.55, 121.02 (2C, Ar), 130.66 (2C, Ar), 141.10, 144.99, 162.73.

Preparation of 1-Deoxo Analogues 75−79. A solution of the appropriate artemisinin analogue (0.35 mmol) in ethyl acetate (6 mL) was mixed with palladium on charcoal (0.02 g 10% w/w) and hydrogenolyzed under a positive pressure of hydrogen for 7 h, the progress of reaction being monitored by TLC. The reaction mixture was filtered, the solvents evaporated under reduced pressure, and the product purified by chromatography on silica gel column, eluting with 10% ethyl acetate−hexanes to afford the corresponding 1-deoxo compounds. Subsequent preparative reverse-phase chromatography on a Waters Prep−6000 system using a 7.8 × 150 mm symmetry column (C-18) and eluting with H_2O:CH_3CN (1:1) provided the highly pure products (>99.9% pure).

(+)-Octahydro-3,6α,9*β*-trimethyl-3,12-epoxy-12*H*-pyrano[4,3*j*]-1,2-benzoxepin-10(3*H*)-one (75) Was Prepared from Artemisinin (1). Yield: 54%. Mp: 107−108 °C. $[\alpha]^{26}_D$ −75.0 ($CHCl_3$, *c* 1.0). ^{1}H NMR ($CDCl_3$): δ 0.94 (d, 3H, J = 5.33 Hz), 1.01 (m, 1H), 1.19 (d, 3H, J = 7.21 Hz), 1.25 (m, 4H), 1.52 (s, 3H), 1.59 (m, 1H), 1.76 (m, 2H), 1.92 (m, 2H), 2.0 (m, 1H), 3.19 (m, 1H), 5.69 (s, 1H). ^{13}C NMR ($CDCl_3$): δ 12.64, 18.60, 22.02, 23.53, 23.99, 32.76, 33.45, 33.97, 35.36, 42.41, 44.61, 82.42, 99.65, 109.23, 171.89. IR (neat) cm^{-1}: 2941, 1748, 1384, 1139, 1009, 1001, 874. HRMS (ESI) *m*/ *z*: calcd for $C_{15}H_{22}O_4Na$ [M + Na]$^+$ 289.1416, found 289.1424 [M + Na]$^+$, 305.1171 [M + K]$^+$. Anal. ($C_{15}H_{22}O_4$): C, H.

(+)-Octahydro-3,6α-dimethyl-3,12-epoxy-9*β*-(3′-(3,5-bis-(trifluoromethyl)phenyl)propyl)-12*H*-pyrano[4,3*j*]-1,2-benzoxepin-10(3*H*)-one (76) was prepared from 27. Yield: 21%. $[\alpha]^{29}_D$ −32.0 ($CHCl_3$, *c* 1.0). ^{1}H NMR ($CDCl_3$): δ 0.93 (d, 3H, J = 4.97 Hz), 1.05 (m, 1H), 1.27 (m, 4H), 1.53 (s, 3H), 1.55−1.70 (m, 2H), 1.79 (m, 4H), 1.91 (m, 2H), 2.05 (m, 2H), 2.77 (m, 2H), 3.01 (m, 1H), 5.68 (s, 1H), 7.64 (s, 2H), 7.71 (s, 1H). ^{13}C NMR ($CDCl_3$): δ 18.55, 22.01, 23.59, 23.96, 26.75, 28.80, 33.39, 33.97, 35.34, 35.57, 37.68, 40.46, 44.65, 54.34, 82.17, 99.31, 109.34, 120.04 (2C), 122.06, 128.49 (2C), 131.43, 131.75, 144.37, 171.04. IR (neat) cm^{-1}: 2921, 1744, 1384, 1287, 1164, 1127, 1013, 894. HRMS (ESI) *m*/*z*: calcd for $C_{25}H_{28}F_6O_4$-Na [M + Na]$^+$ 529.1789, found 529.1769 [M + Na]$^+$, 545.1514 [M + K]$^+$.

(+)-Octahydro-3,6α-dimethyl-3,12-epoxy-9*β*-(3′-(*p*-methanesulfonylphenyl)propyl)-12*H*-pyrano[4,3*j*]-1,2-benzoxepin-10(3*H*)-one (77) Was Prepared from 25. Yield: 32%. Mp: 160−161 °C. $[\alpha]^{25}_D$ +38.0 ($CHCl_3$, *c* 0.5). ^{1}H NMR ($CDCl_3$): δ 0.94 (d, 3H, J = 4.4 Hz), 1.07 (m, 1H), 1.27−1.36 (m, 4H), 1.53 (s, 3H), 1.59−1.69 (m, 2H), 1.78 (m, 4H), 1.85−1.93 (m, 2H), 2.04 (m, 2H), 2.75 (m, 2H), 2.99 (ddd, 1H, J = 4.4, 4.4, 4.4 Hz), 3.05 (s, 3H), 5.68 (s, 1H), 7.40 (d, 2H, J = 8.0 Hz), 7.86 (d, 2H, J = 8.4 Hz). ^{13}C NMR ($CDCl_3$): 18.56, 21.99, 23.57, 23.97, 26.62, 28.73, 33.39, 33.95, 35.32, 35.77, 37.69, 40.38, 44.60, 44.65, 82.16, 99.28, 109.30, 127.51 (2C, Ar), 129.36 (2C, Ar), 138.14, 148.63, 171.14. IR (neat) cm^{-1}: 2929, 1748, 1392, 1307, 1143, 1106, 1029, 869. HRMS (ESI) *m*/*z*: calcd for $C_{24}H_{32}O_6SNa$ [M + Na]$^+$ 471.1817, found 471.1790 [M + Na]$^+$, 487.1535 [M + K]$^+$. Anal. ($C_{24}H_{32}O_6S$·0.5EtOAc): C, H.

(+)-Octahydro-3,6α-dimethyl-3,12-epoxy-9*β*-(3′-(*p*-trifluoromethylphenyl)propyl)-12*H*-pyrano[4,3*j*]-1,2-benzoxepin (78) Was Prepared from 56. Yield: 42%. Mp: 82−83 °C. $[\alpha]^{26}_D$ −7.0 ($CHCl_3$, *c* 1.0). ^{1}H NMR ($CDCl_3$): δ 0.91 (d, 3H, J = 5.2 Hz), 1.02 (m, 1H), 1.17−1.39 (m, 6H), 1.54 (s, 3H), 1.57−1.74 (m, 6H), 1.85 (m, 1H), 1.94 (m, 1H), 2.13 (m, 1H), 2.68 (t, 2H, J = 7.2 Hz), 3.37 (dd, 1H, J = 4.4, 4.4 Hz), 3.94 (dd, 1H, J = 7.2, 7.2 Hz), 5.27 (s, 1H), 7.29 (d, 2H, J = 7.6 Hz), 7.54 (d, 2H, J = 8.0 Hz). ^{13}C NMR ($CDCl_3$): δ 18.85, 22.12, 23.88, 24.01, 29.02, 30.68, 31.65, 34.43, 34.46, 35.41, 35.87, 39.16, 45.77, 62.83, 82.38, 96.43, 107.34, 123.02, 125.22, 125.72, 127.98, 128.30, 128.66, 146.43. IR (neat) cm^{-1}: 2941, 1323, 1160, 1127, 1066, 1001, 886. HRMS (ESI) *m*/*z*: calcd for $C_{24}H_{31}F_3O_3Na$ [M + Na]$^+$ 447.2123, found 447.2113 [M + Na]$^+$, 463.1857 [M + K]$^+$. Anal. ($C_{24}H_{31}F_3O_3$): C, H.

(+)-Octahydro-3,6α-dimethyl-3,12-epoxy-9*β*-(3′-(*m*-chlorophenyl)propyl)-12*H*-pyrano[4,3*j*]-1,2-benzoxepin (79) Was Prepared from 53. Yield: 47%. $[\alpha]^{26}_D$ +30.0 ($CHCl_3$, *c* 0.5). ^{1}H NMR ($CDCl_3$): δ 0.92 (d, 3H, J = 5.6 Hz), 1.03 (m, 1H), 1.17−1.39 (m, 7H), 1.55 (s, 3H), 1.59−1.64 (m, 2H), 1.71 (m, 3H), 1.85 (m, 1H), 1.95 (m, 1H), 2.13 (m, 1H), 2.60 (t, 2H, J = 7.2 Hz), 3.37 (dd, 1H, J = 4.4, 4.8 Hz), 3.94 (dd, 1H, J = 7.2, 6.8 Hz), 5.27 (s, 1H), 7.06 (d, 1H, J = 6.8 Hz), 7.20 (m, 3H). ^{13}C NMR ($CDCl_3$): δ 18.87, 22.14, 23.87, 24.03, 29.05, 30.68, 31.66, 34.44, 34.47, 35.43, 35.72, 39.14, 45.78, 62.90, 82.40, 96.44, 107.34, 125.96, 126.58, 128.48, 129.56, 134.05, 144.37. IR (neat) cm^{-1}: 2933, 1724, 1467, 1279, 1123, 1107, 1074, 1001, 882. HRMS (ESI) *m*/*z*: calcd for $C_{23}H_{31}ClO_3K$ [M + K]$^+$ 429.1599, found 413.1873 [M + Na]$^+$, 429.1596 [M + K]$^+$. Anal. ($C_{23}H_{31}ClO_3$): C, H.

Acknowledgment. This work was supported by CDC Cooperative agreements U50/CCU418839 and UR3/CCU418652. Partial support from USDA under cooperative agreement 58-6408-2-0009 to NCNPR is also acknowledged. Authors are thankful to John Trott for the help in antimalarial testing and Dr. Blake Watkins for helpful suggestions during the preparation of the manuscript.

References

(1) Cumming, J. N.; Ploypradith, P.; Posner, G. H. Antimalarial activity of artemisinin (qinghaosu) and related trioxanes: Mechanism(s) of Action. *Adv. Pharmacol. (San Diego)* **1997**, *37*, 253−297.

(2) Avery, M. A.; Alvim-Gaston, M.; Woolfrey, J. R. Synthesis and structure−activity relationships of peroxidic antimalarials based on artemisinin. *Adv. Med. Chem.* **1999**, *4*, 125−217.

(3) Klayman, D. L. Qinghaosu (artemisinin): An antimalarial drug from China. *Science* **1985**, *228*, 1049−1055.

(4) Robert, A.; Dechy-Cabaret, O.; Cazelles, J.; Meunier, B. From mechanistic studies on artemisinin derivatives to new modular antimalarial drugs. *Acc. Chem. Res.* **2002**, *35*, 167−174.

(5) Wu, Y. How might qinghaosu (artemisinin) and related compounds kill the intraerythrocytic malaria parasite? A chemist's view. *Acc. Chem. Res.* **2002**, *35*, 255−259.

(6) Cazelles, J.; Robert, A.; Meunier, B. Alkylating capacity and reaction products of antimalarial trioxanes after activation by a heme model. *J. Org. Chem.* **2002**, *67*, 609−619.

(7) Wang, D.-Y.; Wu, Y.-L. A possible antimalarial action mode of qinghaosu (artemisinin) series compounds. Alkylation of reduced glutathione by C-centered primary radicals produced from antimalarial compound qinghaosu and 12-(2,4-dimethoxyphenyl)-12-deoxoqinghaosu. *J. Chem. Soc. Chem. Commun.* **2000**, *22*, 2193−2194.

(8) Pandey A. V.; Tekwani, B. L.; Sing, R. L.; Chauhan, V. S. Artemisinin, an endoperoxide antimalarial, disrupts the hemoglobin catabolism and heme detoxification systems in malarial parasite. *J. Biol. Chem.* **1999**, *274*, 19383−19388.

(9) Wu, W.-M.; Wu, Y.; Wu, Y.-L.; Yao Z.-J.; Zhou, C.-M.; Li, Y.; Shan, F. Unified mechanistic framework for the Fe(II)-induced cleavage of qinghaosu and derivatives/analogues. The first spin-trapping evidence for the previously postulated secondary C-4 radical. *J. Am. Chem. Soc.* **1998**, *120*, 3316−3325.

(10) Paitayatat, S.; Tarmchompoo, B.; Thebtatranonth, Y.; Yuthavong, Y. Correlation of antimalarial activity of artemisinin derivatives with binding affinity with ferroprotoporphyrin IX. *J. Med. Chem.* **1997**, *40*, 633−638.

(11) Haynes, R. K.; Vonwiller, S. C. From qinghao, marvelous herb of antiquity, to the antimalarial trioxane qinghaosu−Some remarkable new chemistry. *Acc. Chem. Res.* **1997**, *30*, 73−79.

(12) (a) Meshnick, S. R.; Yang, Y. Z.; Lima, V.; Cuypers, F.; Kamchonwongpaisan, S.; Yuthavong, Y. Iron-dependent free radical generation from the antimalarial agent artemisinin (qinghaosu). *Antimicrob. Agents Chemother.* **1993**, *37*, 1108−1114. (b) Haynes, R. K.; Hung-On, P. H.; Voerste, A. Ring opening of artemisinin (qinghaosu) and dihydroartemisinin and interception of the open hydroperoxides with formation of *N*-oxides−A chemical model for antimalarial action. *Tetrahedron Lett.* **1999**, *40*, 4715−4718.

(13) Bhisutthibhan, J.; Pan, X. Q.; Hossler, P. A.; Walker, D. J. The Plasmodium falciparum translationally controlled tumor protein homologue and its reaction with the antimalarial drug artemisinin. *J. Biol. Chem.* **1998**, *273*, 16192−16198.

(14) Olliaro, P. L.; Haynes, R. K.; Meunier, B.; Yuthavong, Y. Possible modes of action of the artemisinin-type compounds. *Trends Parasitol.* **2001**, *17*, 122−126.
(15) Grellepois, F.; Chorki, F.; Crousse, B.; Ourevitch, M.; Bonnet-Delpon, D.; Jean-Pierre, B. Anhydrodihydroartemisinin and its 10-trifluoromethyl analogue: Access to novel D-ring-contracted artemisinin trifluoromethyl ketones. *J. Org. Chem.* **2002**, *67*, 1253−1260.
(16) Jung, M.; Lee, K.; Kendrick, H.; Robinson, B. L.; Croft, S. L. Synthesis, stability, and antimalarial activity of new hydrolytically stable and water-soluble (+)-Deoxoartelinic acid. *J. Med. Chem.* **2002**, *45*, 4940−4944.
(17) Posner, G. H.; Jeon, H. B.; Ploypradith, P.; Paik, I. H.; Borstnik, K.; Xie, S.; Shapiro, T. A. Orally active, water-soluble antimalarial 3-Aryltrioxanes: Short synthesis and preclinical efficacy testing in rodents. *J. Med. Chem.* **2002**, *45*, 3824−3828.
(18) Hindley, S.; Ward, S. A.; Storr, R. C.; Searle, N. L.; Bray, P. G.; Park, B. K.; Davies, J.; O'Neill, P. M. Mechanism-based design of parasite-targeted artemisinin derivatives: Synthesis and antimalarial activity of new diamine containing analogues. *J. Med. Chem.* **2002**, *45*, 1052−1063.
(19) Chorki, F.; Grellepois, F.; Crousse, B.; Hoang, V. D.; Hung, N. V.; Bonnet-Delpon, D.; Begue, J. P. First synthesis of 10α-(trifluoromethyl)deoxoartemisinin. *Org. Lett.* **2002**, *4*, 757−759.
(20) Liao, X.-B.; Han, J.-Y.; Li, Y. Michael addition of artemisitene. *Tetrahedron Lett.* **2001**, *42*, 2843−2845.
(21) Chorki, F.; Grellepois, F.; Crousse, B.; Ourevitch, M.; Bonnet-Delpon, D.; Begue, J. P. Fluoro artemisinins: Difluoromethylene ketones. *J. Org. Chem.* **2001**, *66*, 7858−7863.
(22) (a) Han, J.; Lee, J. G.; Min, S. S.; Park, S. H.; Angerhofer, C. K.; Cordell, G. A.; Kim, S. U. Synthesis of new artemisinin analogues from artemisinic acid modified at C-3 and C-13 and their antimalarial activity. *J. Nat. Prod.* **2001**, *64*, 1201−1205. (b) Ekthawatchai, S.; Kamchonwongpaisan, S.; Kongsaeree, P.; Tarnchompoo, B.; Thebtaranonth, Y.; Yuthavong, Y. C-16 artemisinin derivatives and their antimalarial and cytotoxic activities: Syntheses of artemisinin monomers, dimers, trimers, and tetramers by nucleophilic additions to artemisitene. *J. Med. Chem.* **2001**, *44*, 4688−4695.
(23) Denis, M. B.; Davis, T. M. E.; Hewitt, S.; Incardona, S.; Nimol, K.; Fandeur, T.; Poravuth, Y.; Lim, C.; Socheat, D. Efficacy and safety of Dihydroartemisinin-Piperaquine (Artekin) in Cambodian children and Adults with uncomplicated Falciparum malaria. *Clin. Infect. Dis.* **2002**, *35*, 1469−1476, and references therein.
(24) (a) Brossi, A.; Venugopalan, B.; Dominguez Gerpe, L.; Yeh, H. J. C.; Flippen-Anderson, J. L.; Buchs, P.; Luo, X. D.; Milhous, W.; Peters, W. Arteether, a new antimalarial drug: Synthesis and antimalarial properties. *J. Med. Chem.* **1988**, *31*, 645−650. (b) Brewer, T. G.; Grate, S. J.; Peggins, J. O.; Weina, P. J.; Petras, J. M.; Levine, B. S.; Heiffer, M. H.; Schuster, B. G. Fatal neurotoxicity of arteether and artemether. *Am. J. Trop. Med. Hyg.* **1994**, *51*, 251−259. (c) Brewer, T. G.; Peggins, J. O.; Grate, S. J.; Petras, J. M.; Levine, B. S.; Weina, P. J.; Swearengen, J.; Heiffer, M. H.; Schuster, B. G. Neurotoxicity in animals due to arteether and artemether. *Trans. R. Soc. Trop. Med. Hyg.* **1994**, *88*, 33−36. (d) Lee, I. S.; Hufford, C. D. Metabolism of antimalarial sesquiterpene lactones. *Pharm., Ther.* **1990**, *48*, 345−355.
(25) Singh, N. P.; Lai, H. Selective toxicity of dihydroartemisinin and holotransferrin toward human breast cancer cells. *Life Sci.* **2001**, *70*, 49−56.
(26) Thomas, E.; Heather, D.; Axel, S.; Hayato, M.; Chitambar, C. R. The anti-malarial artesunate is also active against cancer. *Int. J. Oncol.* **2001**, *18*, 767−773.
(27) Li, Y.; Shan, F.; Wu, J.-M.; Wu, G.-S.; Ding, J.; Xiao, D.; Yang, W.-Y.; Atassi, G.; Leonce, S.; Caignard, D.-H.; Renard, P. Novel antitumor artemisinin derivatives targeting G1 phase of the cell cycle. *Bioorg. Med. Chem. Lett.* **2001**, *11*, 5−8.
(28) Posner, G. H.; Ploypradith, P.; Parker, M. H.; O'Dowd, H.; Woo, S.-H.; Northrop, J.; Krasavin, M.; Dolan, P.; Kensler, T. W.; Xie, S.; Shapiro, T. A. Antimalarial, antiproliferative, and antitumor activities of artemisinin-derived, chemically robust, trioxane dimers. *J. Med. Chem.* **1999**, *42*, 4275−4280.
(29) Beekman, A. C.; Wierenga, P. K.; Woerdenbag, H. J.; Van Uden, W.; Pras, N.; Konings, A. W. T.; El-Feraly, F. S.; Galal, A. M.; Wikstroem, H. V. Artemisinin-derived sesquiterpene lactones as potential antitumour compounds: Cytotoxic action against bone marrow and tumour cells. *Planta Med.* **1998**, *64*, 615−619.
(30) Jung, M. Synthesis and cytotoxicity of novel artemisinin analogues. *Bioorg. Med. Chem. Lett.* **1997**, *7*, 1091−1094.
(31) Liu, C. H.; Zou, W. X.; Lu, H.; Tan, R. X. Antifungal activity of *Artemisia annua* endophyte cultures against phytopathogenic fungi. *J. Biotechnol.* **2001**, *88*, 277−282.
(32) Vikas, D.; Rao, P. S.; Lakshmi, N. M. Antimicrobial activity of artemisinin and its precursors. *Curr. Sci.* **2000**, *78*, 709−713.
(33) Yang, D. M.; Liew, F. Y. Effects of qinghaosu (artemisinin) and its derivatives on experimental cutaneous leishmaniasis. *Parasitology* **1993**, *106*, 7−11.
(34) Kern, P. Leishmaniasis. *Antibiot. Chemother.* **1981**, *30*, 203−223.
(35) De Carvalho, P. B.; Arribas, M. A. D. G.; Ferreira, E. I. Leishmaniasis: What do we know about its chemotherapy? *Rev. Bras. Cienc. Farm.* **2000**, *36*, 69−96.
(36) Loiseau, P. M.; Bories, C. Recent strategies for the chemotherapy of visceral leishmaniasis. *Curr. Opin. Infect. Dis.* **1999**, *12*, 559−564.
(37) Selzer, P. M.; Pingel, S.; Hsieh, I.; Ugele, B.; Chan, V. J.; Engel, J. C.; Bogyo, M.; Russell, D. G.; Sakanari, J. A.; McKerrow, J. H. Cysteine protease inhibitors as chemotherapy: Lessons from a parasite target. *Proc. Natl. Acad. Sci. U.S.A.* **1999**, *96*, 11015−11022.
(38) Moreno, J.; Canavate, C.; Chamizo, C.; Laguna, F.; Alvar, J. HIV-Leishmania infantum co-infection: Humoral and cellular immune responses to the parasite after chemotherapy. *Trans R. Soc. Trop. Med. Hyg.* **2000**, *94*, 328−332.
(39) Kennedy, M. L.; Cortes-Selva, F.; Perez-Victoria, J. M.; Jimenez, I. A.; Gonzalez, A. G.; Munoz, O. M.; Gamarro, F.; Castanys, S.; Ravelo, A. G. Chemosensitization of a multidrug-resistant *Leishmania tropica* line by new sesquiterpenes from *Maytenus magellanica* and *Maytenus chubutensis*. *J. Med. Chem.* **2001**, *44*, 4668−4676.
(40) Berman, J. D.; Grog, I. M. *Leishmania mexicana*: Chemistry and biochemistry of sodium stibogluconate (Pentostam). *Exp. Parasitol.* **1988**, *67*, 96−103.
(41) Brost, P.; Ouellette, M. New mechanisms of drug resistance in parasitic protozoa. *Annu. Rev. Microbiol.* **1995**, *49*, 427−460.
(42) Olliaro, P. L.; Bryceson, A. D. M. Practical progress and new drugs for changing patterns of leishmaniasis. *Parasitol. Today* **1993**, *9*, 323−328.
(43) Thakur, C. P. Comparison of glucose versus fat emulsion in the preparation of amphotericin B for use in kala-azar. *Trans R. Soc. Trop. Med. Hyg.* **1994**, *88*, 689−699.
(44) Dietz, R.; Fagundes, S. M. S.; Brito, E. F.; Milan, E. P.; Fietosa, T. F.; Suassuna, F. A. B.; Fonschiffrey, G.; Ksionski, G.; Dember, J. Treatment of kala-azar in Brazil with Amphocil (amphotericin B cholesterol dispersion) for 5 days. *Trans R. Soc. Trop. Med. Hyg.* **1995**, *89*, 309−311.
(45) (a) Vroman, J. A.; Alvim-Gaston, M.; Avery, M. A. Current progress in the chemistry, medicinal chemistry and drug design of artemisinin based antimalarials. *Curr. Pharm. Design* **1999**, *5*, 101−138. (b) Vroman, J. A.; Elsohly, H. N.; Avery, M. A. Conjugate addition of a cyano-Gilman cuprate to an acrylic acid: Homologation of artemisinic acid and subsequent conversion to 16-butylartemisinin. *Synth. Commun.* **1998**, *28*, 1555−1562. (c) Avery, M. A.; Mehrotra, S.; Bonk, J. D.; Vroman, J. A.; Goins, D. K.; Miller, R. Structure−activity relationships of the antimalarial agent artemisinin. 4. Effect of substitution at C-3. *J. Med. Chem.* **1996**, *39*, 2900−2906. (d) Avery, M. A.; Alvim-Gaston, M.; Rodrigues, C. R.; Barreiro, E. J.; Cohen, F. E.; Sabnis, Y. A.; Woolfrey, J. R. Structure−activity relationships of the antimalarial agent artemisinin. 6. The development of predictive in vitro potency models using CoMFA and HQSAR methodologies. *J. Med. Chem.* **2002**, *45*, 292−303.
(46) (a) Avery, M. A.; Alvim-Gaston, M.; Vroman, J. A.; Wu, B.; Ager, A.; Peters, W.; Robinson, B. L.; Charman, W. Structure−activity relationships of the antimalarial agent artemisinin. 7. Direct modification of (+)-artemisinin and in vivo antimalarial screening of new, potential preclinical antimalarial candidates. *J. Med. Chem.* **2002**, *45*, 4321−4335. (b) Avery, M. A.; Gao, F.; Chong, W. K. M.; Mehrotra, Sanjiv; Milhous, W. K., Structure−activity relationships of the antimalarial agent artemisinin. 1. Synthesis and comparative molecular field analysis of C-9 analogues of artemisinin and 10-deoxoartemisinin. *J. Med. Chem.* **1993**, *36*, 26, 4264−75. (c) Avery, M. A.; Mehrotra, S.; Theresa, L. J.; Bonk, J. D.; Vroman, J. A.; Miller R. Structure−activity relationships of the antimalarial agent artemisinin. 5. Analogues of 10-deoxoartemisinin substituted at C-3 and C-9. *J. Med. Chem.* **1996**, *39*, 4149−4155. (d) Avery, M. A.; Bonk, J. D.; Chong, W. K. M.; Mehrotra, S.; Miller, R.; Milhous, W.; Goins, D. K.; Venkatesan, S.; Wyandt, C.; Khan, I.; Avery, B. A. Structure−activity relationships of the antimalarial agent artemisinin. 2. Effect of heteroatom substitution at O-11: Synthesis and bioassay of *N*-alkyl-11-aza-9-desmethylartemisinins. *J. Med. Chem.* **1995**, *38*, 26, 5038−44. (e) Avery, M. A.; Chong, W. K. M.; Detre, G. Synthesis of (+)-8a,9-secoartemisinin and related analogues. *Tetrahedron Lett.* **1990**, *31*, 13, 1799−802. (f) Avery, M. A.; Fan, P.; Karle, Jean, M.; Miller, R.; Goins, K. Replacement of the nonperoxidic trioxane oxygen atom of artemisinin by carbon: Total synthesis of (+)-13-carbaartemisinin and related structures. *Tetrahedron Lett.* **1995**, *36*, 23, 3965−8. (g) Avery, M. A.; Chong, W. K. M.; Bupp, J. E. Tricyclic analogue of artemisinin: Synthesis and antimalarial activity of (+)-4,5-secoartemisinin and (−)-5-nor-4,5-secoartemisinin. *J. Chem. Soc. Chem. Commun.* **1990**, *21*, 1487−9. (h) Avery, M. A.; Chong, W. K. M.; Bupp, J. Preparation of antimalarial analogues of artemisinin. WO 9114689 A1 19911003, 1991. *Chem. Abstr. 117*, 48951.

(47) Makler, M. T.; Ries, J. M.; Williams, J. A.; Bancroft, J. E.; Piper, R. C.; Gibbins, B. L.; Hinriches, D. J. Parasite lactate dehydrogenase as an assay for *Plasmodium falciparum* drug sensitivity. *Am. J. Trop. Med. Hyg.* **1993**, *48*, 739−741.

(48) (a) Sereno, D.; Roy, G.; Lemesre, J. L.; Papadopoulou, B.; Ouellette, M. DNA transformation of *Leishmania infantum* axenic amastigotes and their use in drug screening. *Antimicrob. Agents Chemother.* **2001**, *45*, 1168−1173. (b) Babich, H.; Borenfreund, E. Cytotoxicity of T2 toxin and its metabolites with the neutral red cell viability assay. *App. Envt Microbiol.* **1991**, *57*, 2101−2103.

(49) Lisgarten, J. N.; Potter, B. S.; Bantuzeko, C.; Palmer, R. A. Structure, absolute configuration, and conformation of the antimalarial compound, artemisinin. *J. Chem. Crystallogr.* **1998**, *28*, 539−543.

(50) *SYBYL 6.9*, Force Field manual; Tripos Inc.: St Louis, MO, p 57.

(51) Gasteiger, J.; Marsili, M. Iterative partial equalization of orbital electronegativity: A rapid access to atomic charges. *Tetrahedron* **1980**, *36*, 3219−3222.

(52) Stewart, J. J. P. *MOPAC 6.0: A general molecular orbital package (QCPE 455)*; Frank J. Seiler Research Laboratory: Colorado Springs, CO.

(53) Bush, B. L.; Nachbar, R. B., Jr. Sample-distance partial least squares: PLS optimized for many variables, with application to CoMFA. *J. Comput-Aided Mol. Des.* **1993**, *7*, 587−619.

(54) Cho, S. J.; Tropsha, A. Cross-validated r^2-guided region selection for comparative molecular field analysis: A simple method to achieve consistent results. *J. Med. Chem.* **1995**, *38*, 1060−1066.

(55) Tropsha, A.; Cho, S. J. *Cross-validated r^2 guided region selection for CoMFA studies. In 3D QSAR methodology: CoMFA and related approaches*; Kubinyi, H., Folkers, G., Martin, Y. C., Eds.; Kluwer Academic Publishers: Dordrecht, The Netherlands, 1998; Vol. III, pp 57−69.

(56) Cramer, R. D., III; Bunce, J. D.; Patterson, D. E. Crossvalidation, bootstrapping, and partial least squares Compared with multiple regression in conventional QSAR studies. *Quant. Struct.-Act. Relat.* **1988**, *7*, 18−25.

(57) Woolfrey, J. R.; Avery, M. A.; Doweyko, A. M. Comparison of 3D quantitative structure−activity relationship models: Analysis of the in vitro antimalarial activity of 154 artemisinin analogues by hypothetical active-site lattice and comparative molecular field analysis. *J. Comput-Aided. Mol. Des.* **1998**, *12*, 165−181.

(58) Cheng, F.; Shen, J.; Luo, X.; Zhu, W.; Gu, J.; Ji, R.; Jiang, H.; Chen, K. Molecular docking and 3-D QSAR studies on the possible antimalarial mechanism of artemisinin analogues. *Bioorg. Med. Chem.* **2002**, *10*, 2883−2891.

(59) Pal, J. K.; Purandare, M. J. Dose-dependent differential effect of hemin on protein synthesis and cell proliferation in *Leishmania donovani* promastigots cultures in vitro. *J. Biosci. (Indian Acad. Sci.)* **2001**, *26*, 225−231.

JM030181Q